UPPSALA
UNIVERSITET

Summation-By-Parts in Time

Carl Sundström, Victor Vadling

Project in Computational Science: Report

8 februari 2020

PROJECT REPORT

Institutionen för informationsteknologi

Contents

Abstract

We develop a high-order accurate numerical method suitable for stiff initial value problems on second order form. The new method is based on finite difference schemes obeying a summation by parts property for discretization in time. Initial conditions are imposed using the projection method. The numerical method is unconditionally stable, high-order accurate and may be directly implemented on second-order initial value problems, without reduction to first order form.

1 Introduction

Partial differential equations (PDEs) of second order in time are essential to the study of wave propagation and dynamical systems in mechanics. A common way of numerically solving such PDEs is to first discretize the initial-boundary value problem (IBVP) in space. The resulting initial value problem (IVP) can then be rewritten as a system of two first-order IVPs. The system is then time-integrated using a suitable numerical method for solving first-order ordinary differential equations (ODEs). A problem this approach leads to is that the number of unknowns increase, as both the solution and the first derivative approximation is computed for each time-step.

A finite elements in time approach for solving time-dependent ODEs was first derived in [1] by Borri et al. in 1985. In 1997 Bottasso showed in [2] that some of the well-known finite elements in time formulations are essentially Runge-Kutta methods. In [10] Nordström et al. developed a high-order accurate numerical method for integrating first-order IVPs in time. This method extends the well-known SBP-SAT technique to the time domain. SBP-SAT combines high-order accurate finite difference schemes following a summation by parts (SBP) property with the simultaneous approximation term (SAT) technique for imposing physical boundary conditions. In [11] Nordström et al. extends the previous work in [10] to handle IVPs on second order form. This proved to be a difficult problem and the method was developed by first rewriting the second-order IVP on first order form.

The aim of this project is to develop and analyse a numerical method (SBP-P) suitable for stiff IVPs on second order form. This will be done by combining high-order accurate SBP operators [5, 4, 7, 3, 6] with the projection (P) method [12, 13, 8].

In Section 2 definitions and conventions are presented in 1D. The hardware, software and definitions related to the numerical simulations are presented in Section 3. In Section 4, the new method is introduced for a well-posed linear system of first-order IVPs. Stability of the method is proven by the derivation of a discrete energy estimate. The SBP-P method is compared with the corresponding SBP-SAT implementation as in [10]. The SBP-P method is also tested on a stiff system of ODEs as well as a first-order hyperbolic PDE. Section 5 presents an extension of the method in Section 4 to second-order IVPs and stability is proven. Additionally, the extended method is studied for a second-order ODE and the dynamic beam equation. Section 6 concludes the work and in Section 7 we present some areas where future work is needed.

2 Definitions and conventions

In this section we define necessary notation and conventions which are used in the present study. The section starts off with continuous definitions followed by discrete definitions.

Let $u = u(x,t) \in L^2[x_l, x_r]$ be a real-valued vector function of d scalar elements defined on the spatial domain $x_l \leq x \leq x_r$ and for time $t_0 \leq t \leq T$. Here x_l and x_r are the left- and right boundaries and t_0 and T are the initial- and final time, respectively. Then the following convention is used for writing $u = (u^{(1)}, u^{(2)}, ..., u^{(d)})^T$, where each element $u^{(i)} = u^{(i)}(x,t)$ is a continuous function for $i = 1, 2, ..., d$.

Definition 2.1. A continuous inner product for the real-valued vector function u is

$$(u, Au) \equiv \int_{x_l}^{x_r} u^T A u \, \mathrm{d}x, \tag{1}$$

where A is a positive definite symmetric $d \times d$-matrix.

Definition 2.2. The corresponding continuous norm for the inner product defined in 2.1 is

$$\|u\|_A^2 \equiv (u, Au), \tag{2}$$

which for a positive definite matrix A is zero if and only if all d elements of u are zero.

Let now the spatial domain be divided into m subintervals, defined by the $m+1$ grid points $x = (x_0, x_1, ..., x_{m-1}, x_m)^T$, such that $x_i = x_l + ih$, where $h = (x_r - x_l)/m$ for $i = 0, 1, ..., m$. Then the semi-discrete vector function $v = v(t) \in \mathbb{R}^{d(m+1)}$ corresponding to the scalar function $u = u(x,t)$ (when $d = 1$) is written as

$$v = v(t) \equiv (v_0, v_1, ..., v_{m-1}, v_m)^T, \tag{3}$$

where each element v_i in v is the time-dependent semi-discrete solution at the corresponding grid points x_i in x. Similarly, the time domain may be divided into n subintervals, defined by the $n+1$ grid points $t = (t_0, t_1, ..., t_{n-1}, t_n)^T$, such that $t_j = t_0 + jk$, where $k = (T - t_0)/n$ for $j = 0, 1, ..., n$. Then the semi-discrete vector function is instead given by $v = v(x) \in \mathbb{R}^{d(n+1)}$ and is written similarly as

$$v = v(x) \equiv (v^{(0)}, v^{(1)}, ..., v^{(n-1)}, v^{(n)})^T, \tag{4}$$

where each element $v^{(j)}$ in v is the space-dependent semi-discrete solution at the corresponding grid points t_i in t. The full discretization in time and space is defined, using the conventions for the two separate semi-discretizations in (3) and (4), as

$$w \equiv (w_0^{(0)}, w_1^{(0)}, ..., w_m^{(0)}, ..., w_0^{(n)}, w_1^{(n)}, ..., w_m^{(n)})^T. \tag{5}$$

When working with the fully discrete vector w it is convenient to use the Kronecker product, which is defined as follows:

$$A \otimes B = \begin{pmatrix} a_{11}B & \dots & a_{1m}B \\ \vdots & \ddots & \vdots \\ a_{m1}B & \dots & a_{mm}B \end{pmatrix}, \tag{6}$$

if $A \in \mathbb{C}^{m \times m}$ and $B \in \mathbb{C}^{n \times n}$ are matrices with elements a_{ij} and b_{ij}, respectively. The mixed-product property $(A \otimes B)(C \otimes D) = (AC \otimes BD)$ as well as the transpose-inversion property $(A \otimes B)^{T-1} = (A^{T-1} \otimes B^{T-1})$ are two properties of the Kronecker product which will be frequently used in the present study.

Definition 2.3. A discrete inner product for the fully-discrete vector $w \in \mathbb{R}^{(n+1)(m+1)}$ is:

$$\langle w, (A \otimes B)w \rangle \equiv w^T (A \otimes B) w, \tag{7}$$

where $(A \otimes B) \in \mathbb{C}^{(n+1)(m+1) \times (n+1)(m+1)}$ is a positive definite symmetric matrix.

Definition 2.4. The corresponding discrete norm for the inner product in 2.3 is:

$$\|w\|_{A \otimes B}^2 \equiv \langle w, (A \otimes B)w \rangle, \tag{8}$$

if $(A \otimes B)$ is a positive definite symmetric real matrix.

The following vector and matrix notation are central for the coming analysis:

$$\begin{aligned} \mathbf{1} &= (1, 1, ..., 1)^T, & e_0 &= (1, 0, ..., 0)^T, \\ \mathbf{0} &= (0, 0, ..., 0)^T, & e_k &= (0, 0, ..., 1)^T, \\ & & i &= 0, 1, ..., k, \end{aligned} \tag{9}$$

where k is a positive integer and $e_i \in \mathbb{R}^{k+1}$ is a unit vector with a one at the ith element.

2.1 Summation by parts operators

The SBP operators used in the present study consist of two finite difference stencils of different accuracy order. They use one type of finite difference stencil at the boundaries (boundary closure) and another for the interior of the domain (interior stencil). A $2p$-accurate SBP operator consists of p-accurate stencils at the boundaries (boundary accuracy) and a $2p$-accurate stencil in the interior (interior accuracy). Similarly, a $2p+1$-accurate SBP operator has boundary accuracy p and interior accuracy $2p+1$. [4, 5]

Following the conventions for semi-discrete vector functions in (3) and (4), a first derivative central SBP operator is defined for $k+1$ grid points, as in [5]:

$$D_1 = H^{-1}\left(Q + \frac{1}{2}(e_k e_k^T - e_0 e_0^T)\right), \tag{10}$$

where $H \in \mathrm{R}^{(k+1)\times(k+1)}$ is a symmetric positive definite matrix which defines a discrete norm such that $\mathbf{1}^T H \mathbf{1} = 1$, independently of the $k+1$ number of grid points. Similarly, a first derivative upwind SBP operator is defined as in [4]:

$$D_\pm = H^{-1}\left(Q_\pm + \frac{1}{2}(e_k e_k^T - e_0 e_0^T)\right). \tag{11}$$

The central first derivative SBP operators satisfy $Q + Q^T = 0$, while the upwind operators satisfy $Q_+ + Q_-^T = 0$ as well as $Q_+ + Q_+^T = \frac{1}{2}S$, where S is a negative semi-definite matrix. Finally, a general SBP operator for approximating the first derivative is denoted:

$$D = \begin{pmatrix} d_0^T \\ \vdots \\ d_k^T \end{pmatrix}, \tag{12}$$

where $d_i = e_i^T D$ is a first derivative approximator at the ith grid point. [4, 5]

2.2 The projection method

Here, some necessary operators regarding the projection method will be presented. In order to do this, we consider the second-order linear IBVP in one spatial dimension:

$$\begin{aligned} Au_{tt} + Bu_t + Ru = F(x,t), &\quad x_l < x < x_r, &\quad t > 0, \\ L_l^T u(0,t) = g_l(t), &\quad x = x_l, &\quad t > 0, \\ L_r^T u(x_r,t) = g_r(t), &\quad x = x_r, &\quad t > 0, \\ L_{ic}^T u(x,0) = f_c(x), &\quad x_l < x < x_r, &\quad t = 0, \end{aligned} \tag{13}$$

where A and B are scalar coefficients, R is a linear differential operator, $F(x,t) \in \mathbb{R}$ is a forcing function, $g_l(t) \in \mathbb{R}^{d_l}$, $g_r(t) \in \mathbb{R}^{d_r}$ are boundary data and $f_c(x) \in \mathbb{R}^2$ is initial data. Finally $L_l \in \mathbb{R}^{1\times d_l}$, $L_r \in \mathbb{R}^{1\times d_r}$ are boundary operators and $L_{ic} \in \mathbb{R}^{1\times 2}$ is the initial condition operator.

To numerically approximate the solution to the linear IBVP in (13), one would typically start off by discretizing the problem in space to yield a linear second-order IVP. This can be done using SBP operators to approximate the linear differential operator R. The boundary treatment is then handled using the projection method, which requires a projection operator P_x defined in accordance with [8, 12, 13] as

$$P_x = I_m - H_x^{-1} L_x \left(L_x^T H_x^{-1} L_x\right)^{-1} L_x^T, \tag{14}$$

where $I_m \in \mathbb{R}^{(m+1)\times(m+1)}$ denotes the identity matrix and $H_x \in \mathbb{R}^{(m+1)\times(m+1)}$ is the symmetric and positive definite matrix of the corresponding SBP operator defined on a grid with $m+1$ grid points. Finally, $L_x \in \mathbb{R}^{(m+1)\times(d_l+d_r)}$ is the discrete full boundary operator approximating (L_l, L_r) and satisfies $L_x^T v(t) = (g_l(t), g_r(t))^T$.

The resulting IVP may then be discretized similarly by the introduction of the corresponding projection operator in time. It is defined as

$$P_t = I_n - H_t^{-1} L_t \left(L_t^T H_t^{-1} L_t \right)^{-1} L_t^T, \tag{15}$$

where $I_n \in \mathbb{R}^{(n+1)\times(n+1)}$ denotes the identity matrix and $H_t \in \mathbb{R}^{(n+1)\times(n+1)}$ the symmetric and positive definite matrix of the corresponding SBP operator defined on a grid with $n+1$ grid points. Moreover, $L_t \in \mathbb{R}^{(n+1)\times 2}$ is the discrete full initial condition operator approximating L_{ic} which satisfies $L_t^T v(x) = f_c(x)$.

Remark. *The size of the discrete full initial condition operator L_t is determined by the number of initial conditions needed to guarantee a well-posed IBVP. This number is further determined by the leading derivative in time. For a leading first derivative only one initial condition is required and the operator L_t would in this case have size $(n+1) \times 1$.*

3 Specifications for numerical study

A computer with the following hardware specifications has been used for numerical simulations made in this project: Intel(R) Core(TM) i7-9700K CPU @ 3.60GHz, 16.0 GB RAM, running on the operating system Windows 10 Home v.1903 64-bit.

The software used was `MATLAB` R2019a. In `MATLAB`, the "\"-operator was used to solve linear equation systems (produced by the SBP-P method). The condition number of matrices was computed using the *cond*-function. Finally eigenvalues- and eigenvectors have been obtained using the *eig*-function.

The absolute error is defined as

$$|u - w| \equiv \sqrt{\left(u^{(n)} - w^{(n)}\right)^2}, \tag{16}$$

and was used when studying the numerical solution to scalar ODEs. It was computed between the analytical solution $u^{(n)} \in \mathbb{R}$ and the numerical approximation $w^{(n)} \in \mathbb{R}$ at the final time t_n. The discrete l^2-error was further used when studying semi-discrete PDEs. It is defined as

$$l^2(u - w) \equiv \|u^{(n)} - w^{(n)}\|_{H_x}, \tag{17}$$

where $u^{(n)} \in \mathbb{R}^{m+1}$ and $w^{(n)} \in \mathbb{R}^{m+1}$ is the discrete solution at the final time t_n. The convergence rate (in this study denoted q) was evaluated with the absolute error as

$$q = \log_{10}\left(\frac{|u - w^{(n_1)}|}{|u - w^{(n_2)}|} \right) / \log_{10}\left(\frac{n_1}{n_2} \right), \tag{18}$$

for two different number of grid points n_1 and n_2. Similarly, the convergence rate with the l^2-norm is defined as

$$q = \log_{10}\left(\frac{\|u^{(n_1)} - w^{(n_1)}\|_{H_x}}{\|u^{(n_2)} - w^{(n_2)}\|_{H_x}} \right) / \log_{10}\left(\frac{n_1}{n_2} \right). \tag{19}$$

4 SBP in time: First derivative

In this Section, we present a stable numerical method for handling linear first-order IVPs on the form

$$\begin{aligned} Av_t + Bv &= F_c(t), \quad t > 0, \\ L_c^T v &= f_c, \qquad t = 0, \end{aligned} \tag{20}$$

where $v = v(t) \in \mathbb{R}^{m+1}$ is the time-dependent exact solution. The coefficients $A, B \in \mathbb{R}^{(m+1)\times(m+1)}$ are matrices, resulting in the more general problem which may come from a space discretization of a IBVP using i.e. a finite difference or finite element method. Moreover, $F(t) \in \mathbb{R}^{m+1}$ is the forcing term and $L_c \in \mathbb{R}^{(m+1)\times(m+1)}$ is the linear initial condition operator, which defines the initial configuration together with the initial data $f_c \in \mathbb{R}^{m+1}$. Using the definition for a first-order IVP in equation (20), the SBP-P discretization is defined for the problem as in Definition 4.1.

Definition 4.1. Let D be a first derivative SBP operator based on the symmetric positive definite matrix H. Let further P_t be the projection operator created as in equation (15) and $L_t \in \mathbb{R}^{n+1}$ the discrete linear initial condition operator satisfying $(L_t^T \otimes I_m)w = f$, for $f \in \mathbb{R}^{m+1}$. Then the SBP-P discretization of the IVP in (20) is defined as

$$\begin{aligned}(P_t \otimes I_m)\Big((D \otimes A)\big((P_t \otimes I_m)w + ((I_n - P_t) \otimes I_m)\tilde{f}\big) \\ +(I_n \otimes B)\big((P_t \otimes I_m)w + ((I_n - P_t) \otimes I_m)\tilde{f}\big)\Big) \\ = (P_t \otimes I_m)F - \sigma_t\big((I_n - P_t) \otimes I_m\big)(w - \tilde{f}), \quad \sigma_t > 0,\end{aligned} \tag{21}$$

where $w \in \mathbb{R}^{(m+1)(n+1)}$ is the fully-discrete numerical solution, $I_n \in \mathbb{R}^{(n+1)\times(n+1)}$ and $I_m \in \mathbb{R}^{(m+1)\times(m+1)}$ are identity matrices and k is the time-step. Finally $F \in \mathbb{R}^{(m+1)(n+1)}$ is the fully discrete forcing term, $\tilde{f} \in \mathbb{R}^{(m+1)(n+1)}$ a discrete vector satisfying $(L_t^T \otimes I_m)\tilde{f} = f$ and σ_t a positive constant.

Remark. *The discrete vector $\tilde{f}$ is only introduced for notational convenience and is never used in a practical implementation. Instead it should be noticed that $I_n - P_t = H^{-1}L_t(L_t^T H^{-1}L_t)^{-1}L_t^T$, such that $((I_n - P_t) \otimes I_m)\tilde{f} = (R \otimes I_m)f$ where R is defined as $R = H^{-1}L_t(L_t^T H^{-1}L_t)^{-1}$.*

4.1 Stability of discretization

For the SBP-P discretization in Definition 4.1 to be stable, it is required that D is a first derivative SBP operator. In addition, the underlying IVP in equation (20) also has to be well posed. This is fulfilled in parts by setting the correct number of initial conditions, but the coefficient matrices A and B also need to fulfill certain requirements.

4.1.1 Continuous energy estimate

We can analyse these requirements by using the steps of the energy method. We therefore set $f_c = F_c(t) = 0$ in the analysis and proceed by multiplying equation (20) by the complex conjugate transpose v^* from the left to obtain

$$\langle v, Av_t\rangle + \langle v, Bv\rangle = 0. \tag{22}$$

Adding the complex conjugate transpose of the expression in equation (22) to itself yields

$$\langle v, Av_t\rangle + \langle v_t, A^*v\rangle + \langle v, Bv\rangle + \langle v, B^*v\rangle = 0. \tag{23}$$

From the expression in equation (23), it can be seen that the energy rate is obtained by restricting the matrix A to $A = A^*$. By using the product differentiation rule then leads to the energy rate

$$\begin{aligned}\langle v, Av_t\rangle + \langle v_t, A^*v\rangle + \langle v, Bv\rangle + \langle v, B^*v\rangle &= \frac{d}{dt}\langle v, Av\rangle + \langle v, (B + B^*)v\rangle \\ &= \frac{d}{dt}\|v\|_A^2 + \|v\|_{B+B^*}^2 \\ &= 0.\end{aligned} \tag{24}$$

In order for the IVP in equation (20) to be well posed, the energy rate in (24) needs to be non-positive. This is satisfied if $A = A^* > 0$ and $B + B^* \geq 0$. Integrating the expression in equation (24) over time then results in the following energy estimate:

$$\begin{aligned}\|v(T)\|_A^2 + \int_{t_0}^{T} \|v\|_{B+B^*}^2 \mathrm{d}t &= \|v(t_0)\|_A^2 \\ &= \|f_c\|_A^2 \\ &= 0.\end{aligned} \tag{25}$$

It may be concluded, from the energy estimate obtained in equation (25), that the IVP in (20) is well posed if $A = A^* > 0$, $B + B^* \geq 0$ and $v(t_0)$ is set to the initial data f_c.

4.1.2 Discrete energy estimate

Knowing that the underlying IVP is well posed, it remains to show that the numerical solution w is bounded in order to guarantee stability of the SBP-P method. This can be proved using the discrete energy method to derive a discrete energy estimate. Before doing this, we introduce two lemmas which will be useful when proving the stability of the SBP-P method on the IVP in equation (20).

Lemma 4.1. *If D_1 is a central first derivative SBP operator, defined in accordance with [5] as in equation (10) on a grid of $n+1$ grid points, then the following relationship holds:*

$$HD_1 + D_1^T H^T = e_n e_n^T - e_0 e_0^T. \tag{26}$$

Proof. Use the definition of a central first derivative SBP operator, the symmetry property of the diagonal matrix H and the requirement $Q + Q^T = 0$ imposed on the matrix Q:

$$\begin{aligned} HD_1 + D_1^T H^T &= HH^{-1}\left(Q + \frac{1}{2}(e_n e_n^T - e_0 e_0^T)\right) + \left(Q^T + \frac{1}{2}(e_n e_n^T - e_0 e_0^T)\right) HH^{-1} \\ &= Q + Q^T + e_n e_n^T - e_0 e_0^T \\ &= e_n e_n^T - e_0 e_0^T. \end{aligned} \tag{27}$$

□

Lemma 4.2. *If D_- is an upwind first derivative SBP operator, defined in accordance with [4] as in (11) on a grid of $n+1$ grid points, then the following relationship holds:*

$$HD_- + D_-^T H^T = e_n e_n^T - e_0 e_0^T - \frac{S}{2}, \tag{28}$$

where $S \leq 0$ is a negative semi-definite matrix.

Proof. Use the definition of an upwind first derivative SBP operator D_-, the symmetry property of the diagonal matrix H and the requirement $Q_- + Q_-^T = -\frac{S}{2}$ imposed on the matrix Q_-:

$$\begin{aligned} HD_- + D_-^T H^T &= HH^{-1}\left(Q_- + \frac{1}{2}(e_n e_n^T - e_0 e_0^T)\right) + \left(Q_-^T + \frac{1}{2}(e_n e_n^T - e_0 e_0^T)\right) HH^{-1} \\ &= Q_- + Q_-^T + e_n e_n^T - e_0 e_0^T \\ &= e_n e_n^T - e_0 e_0^T - \frac{S}{2}. \end{aligned} \tag{29}$$

□

With Lemma 4.1 and 4.2 in our toolbox, we will now proceed to derive a discrete energy estimate for the central and upwind SBP operators. Multiply therefore equation (21) by w^*H from the left and set $\tilde{f}$ and F to zero to get

$$w^*(P_t^T HDP_t \otimes A)w + w^*(P_t^T HP_t \otimes B)w = -\sigma_t w^*(H(I_n - P_t) \otimes I_m)w. \tag{30}$$

Adding the complex conjugate transpose of the result from equation (30) to itself and utilizing the projection operator property $HP_t = P_t^T H$ described in [8, 12] leads to

$$w^*(P_t^T[HD + D^T H^T]P_t \otimes A)w + w^*(P_t^T HP_t \otimes [B + B^*])w = -2\sigma_t w^*(H(I_n - P_t) \otimes I_m)w. \tag{31}$$

By introducing the projected solution $\tilde{w} \equiv (P_t \otimes I_m)w$ we may simplify the expression in equation (31) as follows:

$$\begin{aligned} \tilde{w}^*([HD + D^T H^T] \otimes A)\tilde{w} + \tilde{w}^*(H \otimes [B + B^*])\tilde{w} &= -2\sigma_t w^*(H(I_n - P_t) \otimes I_m)w \\ &= -2\sigma_t w^*(H(H^{-1}L_t(L_t^T H^{-1}L_t)^{-1}L_t^T) \otimes I_m)w \\ &= -2\sigma_t \left((L_t^T \otimes I_m)w\right)^* \left((L_t^T H^{-1}L_t)^{-1} \otimes I_m\right)\left((L_t^T \otimes I_m)w\right). \end{aligned} \tag{32}$$

The term in the r.h.s. of (32) is a quadratic term in the initial conditions (recall $(L_t^T \otimes I_m)w = f$ from Definition 4.1) and is zero if the initial condition is consistent with possible boundary conditions. If the initial condition is set inconsistently with the boundary conditions, this term provides damping of the resulting initial error at the boundaries. Using Lemma 4.1 and 4.2 it is now straightforward to deduce the following two discrete energy estimates:

$$\begin{aligned} &(\text{central } D_1): \quad \|\tilde{w}^{(n)}\|_A^2 + \|\tilde{w}\|_{H\otimes(B+B^*)}^2 = \|\tilde{w}^{(0)}\|_A^2 + PT_h, \\ &(\text{upwind } D_-): \quad \|\tilde{w}^{(n)}\|_A^2 + \|\tilde{w}\|_{H\otimes(B+B^*)}^2 = \|\tilde{w}^{(0)}\|_A^2 + PT_h + AD_h. \end{aligned} \tag{33}$$

Comparing the discrete energy estimates in equation (33) to the continuous estimate in (25), it is evident that the SBP-P discretization exactly mimics the IVP in equation (20). In the discrete estimates, there are however two additional terms:

$$\begin{aligned} PT_h &\equiv -2\sigma_t \left((L_t^T \otimes I_m)w\right)^* \left((L_t^T H^{-1} L_t)^{-1} \otimes I_m\right) \left((L_t^T \otimes I_m)w\right), \\ AD_h &\equiv \frac{1}{2}\tilde{w}^*(S \otimes A)\tilde{w}, \end{aligned} \tag{34}$$

which both provide damping. Here PT_h comes from the penalty term in the r.h.s. of equation (32) and AD_h from the additional requirement $Q_- + Q_-^T = -S/2$ in the definition of an upwind first derivative SBP operator (see further in [4] and in equation (11)).

4.2 SBP-SAT vs. SBP-P

In this section, the SBP-SAT and SBP-P method are implemented on the following linear first-order ODE in time:

$$\begin{aligned} u_t + \alpha u = 0, \quad t > 0, \\ u = f, \quad t = 0, \end{aligned} \tag{35}$$

where $u = u(t) \in \mathbb{R}$ is the analytical solution $u = fe^{-\alpha t}$ and the coefficient $\alpha \in \mathbb{R}$ is set to $\alpha = 1$ in accordance with the energy estimate in equation (25). Finally the initial data $f \in \mathbb{R}$ is set to $f = 1$. This exact problem has been studied for $0 \leq t \leq 1$ using SBP-SAT in [10] and we therefore reproduce the results using their choice of penalty parameter $\tau = -1$. The SBP-SAT discretization of (35) is then given as:

$$Dw = -\alpha w + \tau H^{-1} e_0 (e_0^T w - f). \tag{36}$$

As (35) is a special case of (20) with $m = 0$, the corresponding SBP-P discretization is given directly by Definition 4.1 by setting $A = 1$, $B = \alpha$ and $F = 0$ as

$$P_t D(P_t w + (I_n - P_t)\tilde{f}) = -\alpha P_t w - \sigma_t (I_n - P_t)(w - \tilde{f}), \tag{37}$$

where $\sigma_t = 1$.

4.2.1 Numerical results

In this section, the results from a convergence study are presented for the SBP-SAT and SBP-P method on the model problem in (35). The study was made using central SBP operators of 2nd, 4th and 6th accuracy order and the results were obtained at time $t = 1$. The results are presented in Table 1 for the SBP-SAT method and in Table 2 for the SBP-P method.

Table 1: The absolute error in 10-logarithm and convergence rate of the numerical SBP-SAT solution w, using central SBP operators of accuracy orders 2, 4 and 6.

n	$\log_{10}\lvert u-w\rvert$	$q_{(2)}$	$\log_{10}\lvert u-w\rvert$	$q_{(4)}$	$\log_{10}\lvert u-w\rvert$	$q_{(6)}$
10	-3.1252	-	-5.5834	-	-1.6020	-
20	-3.7709	-2.15	-6.9500	-4.54	-9.6436	-26.71
50	-4.5930	-2.07	-8.6405	-4.25	-12.3802	-6.88
100	-5.2038	-2.03	-9.8779	-4.11	-14.4361	-6.83
200	-5.8102	-2.01	-11.0990	-4.06	-14.5835	-0.49

Table 2: The absolute error in 10-logarithm and convergence rate of the numerical SBP-P solution w, using central SBP operators of accuracy order 2, 4 and 6.

n	$\log_{10}\lvert u-w\rvert$	$q_{(2)}$	$\log_{10}\lvert u-w\rvert$	$q_{(4)}$	$\log_{10}\lvert u-w\rvert$	$q_{(6)}$
10	-2.6907	-	-4.0302	-	-1.6397	-
20	-3.3385	-2.15	-4.9544	-3.07	-6.3503	-15.65
50	-4.1610	-2.07	-6.1636	-3.04	-8.0468	-4.26
100	-4.7719	-2.03	-7.0721	-3.02	-9.2923	-4.14
200	-5.3783	-2.01	-7.9779	-3.01	-10.5187	-4.07

Remark. *A central first derivative SBP operator is divided into three sections; [boundary, interior, boundary]. If the interior finite-difference stencil has accuracy order* $2p$*, then the boundary closure is of order* p*. These results show that the SBP-SAT method in time yields a convergence rate related to the accuracy order* $2p$*. In contrast, the SBP-P method in time yields a lower convergence rate related to the boundary closure of* $p+1$*. The SBP-SAT method has however yet to be directly implemented for a second-order IVP, which has proved to be a difficult task in [11].*

4.3 First-order stiff ODE system

In this section, we consider a first-order time-dependent ODE system given by

$$\begin{aligned} u_t + Au &= 0, \quad t > 0, \\ u &= f, \quad t = 0, \end{aligned} \tag{38}$$

where $u = (u^{(1)}, u^{(2)})^T$ is the solution, $f = (f_1, f_2)^T$ is the initial condition for $u^{(1)}$ and $u^{(2)}$, respectively. Finally $A = A^T$ is a complex matrix defined as

$$A = \begin{bmatrix} \alpha & \gamma \\ \gamma & \beta \end{bmatrix}, \tag{39}$$

where the elements are set to $\alpha = -50i$, $\beta = 10000$ and $\gamma = -100i$. This choice of matrix A leads to the eigenvalues

$$\begin{aligned} \lambda_1 &\approx 1.000 - 50.005i, \\ \lambda_2 &\approx 9999.000 + 0.005i, \end{aligned} \tag{40}$$

which correspond to one quickly and one slowly damped solution $u^{(2)}$ and $u^{(1)}$, respectively. The analytical solution to this problem is

$$u(t) = c_1 e^{-\lambda_1 t} r_1 + c_2 e^{-\lambda_2 t} r_2, \tag{41}$$

where $r_1 \in \mathbb{R}^2$ and $r_2 \in \mathbb{R}^2$ are the eigenvectors corresponding to the eigenvalues λ_1 and λ_2, respectively [9]. Then $c = (c_1, c_2)^T$ is the solution to the linear equation system $(r_1, r_2)c = f$.

Multiplying (38) by u^* from the left, adding the complex conjugate result to itself and integrating over time leads to the following continuous energy estimate:

$$\begin{aligned}
&\int_{t_0}^{T} (u^* u_t + u_t^* u + u^* A u + u^* A^* u) \mathrm{d}t \\
&= \int_{t_0}^{T} \left(\frac{d}{dt}(u^* u) + u^*(A + A^*)u \right) \mathrm{d}t \\
&= \int_{t_0}^{T} \left(\frac{d}{dt}(u^* u) + 2\beta (u^{(2)})^* u^{(2)} \right) \mathrm{d}t \\
&= |u(T)|^2 - |u(t_0)|^2 + 2\beta \int_{t_0}^{T} |u^{(2)}|^2 \mathrm{d}t = 0,
\end{aligned} \tag{42}$$

where $|u|^2 \equiv u^* u$. Inserting the specified value for the initial condition leads to the simplified expression

$$|u(T)|^2 + 2\beta \int_{t_0}^{T} |u^{(2)}|^2 \mathrm{d}t = 0. \tag{43}$$

As can be seen, the IVP in equation (38) is a well-posed problem if $\beta \geq 0$. The corresponding stable SBP-P discretization may then be written out (in accordance with Definition 4.1) as follows:

$$\begin{aligned}
(P_t \otimes I_2)\Big(&(D \otimes I_2)\big((P_t \otimes I_2)w + ((I_n - P_t) \otimes I_2)\tilde{f}\big) \\
&+ (I_n \otimes A)\big((P_t \otimes I_2)w + ((I_n - P_t) \otimes I_2)\tilde{f}\big)\Big) \\
&= -\sigma_t \big((I_n - P_t) \otimes I_2\big)(w - \tilde{f}), \quad \sigma_t > 0,
\end{aligned} \tag{44}$$

where I_2 is the 2×2 identity matrix and the projection operator P_t is created as in (15) with the discrete linear initial condition operator $L_t \equiv e_0$. The numerical solution $w \in \mathrm{R}^{2(n+1)}$ thus satisfies $(L_t^T \otimes I_2)w = f$. A discrete energy estimate can be obtained for the SBP-P discretization in (44). This is done by multiplying $w^* H$ from the left and adding the complex conjugate transpose of the resulting expression to itself as follows

$$\begin{aligned}
\tilde{w}^*([HD + D^T H^T] \otimes I_2)\tilde{w} + \tilde{w}^*(H \otimes (A + \acute{A}^*))\tilde{w} \\
&= \tilde{w}^*([HD + D^T H^T] \otimes I_2)\tilde{w} + 2\beta \|\tilde{w}^{(2)}\|_H^2 \\
&= -2\sigma_t w^*(H(I_n - P_t) \otimes I_2)w.
\end{aligned} \tag{45}$$

The following convention $w = (w_0^{(1)}, w_0^{(2)}, ..., w_i^{(1)}, w_i^{(2)}, ..., w_n^{(1)}, w_n^{(2)})^T$ is temporarily adopted and $\tilde{w} = (P_t \otimes I_2)w$ is the projected solution. A discrete energy estimate is then derived using Lemma 4.1 and 4.2 and is given on the following form:

$$\begin{aligned}
&(\text{central } D_1): \quad |\tilde{w}_n|^2 - |\tilde{w}_0|^2 + 2\beta \|\tilde{w}^{(2)}\|_H^2 = PT_h, \\
&(\text{upwind } D_-): \quad |\tilde{w}_n|^2 - |\tilde{w}_0|^2 + 2\beta \|\tilde{w}^{(2)}\|_H^2 = PT_h + AD_h,
\end{aligned} \tag{46}$$

where $\tilde{w}_i = (\tilde{w}_i^{(1)}, \tilde{w}_i^{(2)})^T$ and the damping terms in the r.h.s. are given as:

$$\begin{aligned}
PT_h &\equiv -2\sigma_t \left((L_t^T \otimes I_2)w\right)^* \left((L_t^T H^{-1} L_t)^{-1} \otimes I_2\right) \left((L_t^T \otimes I_2)w\right), \\
AD_h &\equiv \frac{1}{2} \tilde{w}^* (S \otimes I_2)\tilde{w}.
\end{aligned} \tag{47}$$

The discrete energy estimate thus mimics the continuous estimate and the numerical solution is bounded.

4.3.1 Numerical results

In this Section we will present the numerical results obtained using the SBP-P method in equation (44) on the IVP defined in (38). A visual comparison between the numerical and exact solution is given in Figure 1, where the time-domain is divided into 5001 grid points and (38) has been discretized using a 9th order accurate upwind SBP operator with optimal boundary closure (see [6] for further details about the operator). The condition number is computed and shown in Figure 2 for the resulting linear equation system from the SBP-P discretization in (44). The condition number is computed in 2-norm for different number of grid points in time and compared for upwind and central SBP operators with different accuracy orders.

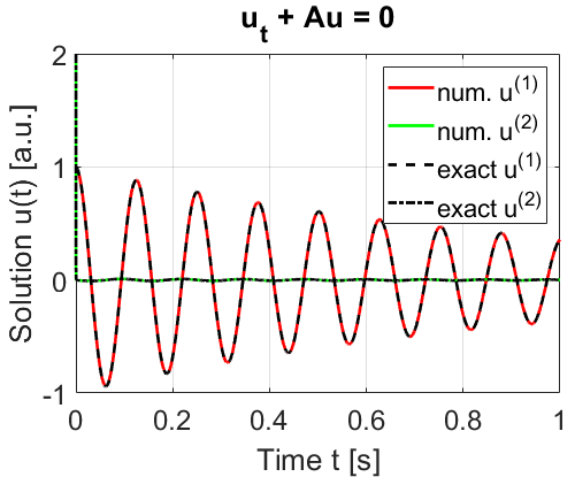

Figure 1: The numerical and analytical real solutions to the homogeneous ode system in equation (38) plotted against time for $t = 0$ to $t = 1$ seconds.

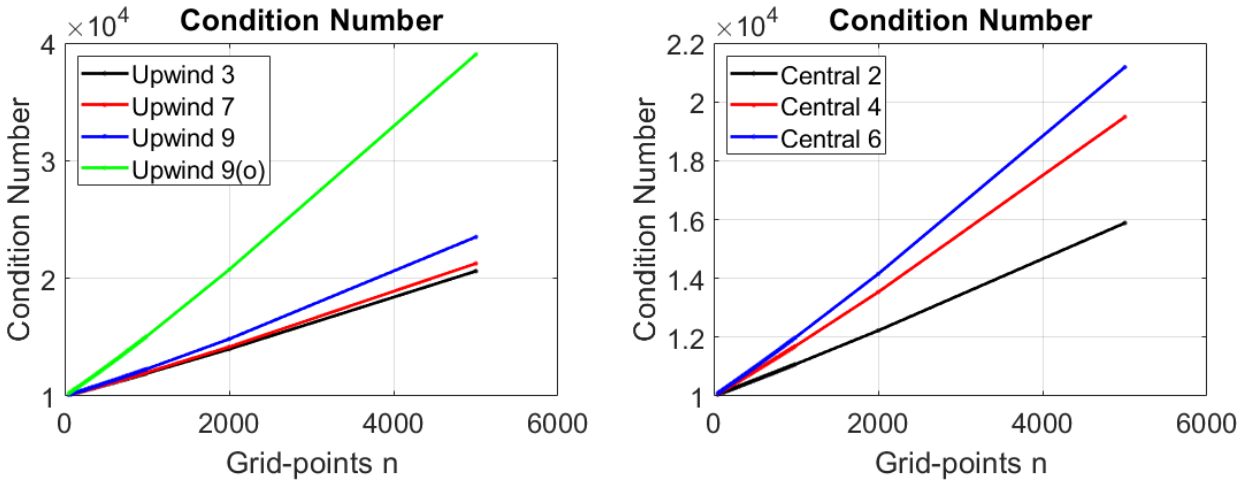

(a) (b)

Figure 2: The condition number (2-norm) plotted against the number of grid points n in (a) using upwind- and (b) using central SBP operators.

Remark. *The condition number is increasing linearly with increasing number of grid points in the time-discretization (see Figure 2). It should also be noted that the condition number increases with the accuracy order of the finite-difference stencil used in the different SBP operators.*

A convergence study has been made for the SBP-P method and the results are presented in Table 3, comparing 3rd, 7th and 9th order accurate upwind SBP operators. An additional 9th order accurate SBP operator was also included in Table 3 and is denoted 9(o) [6]. In Table 4 the corresponding results

are shown, comparing 2nd, 4th and 6th order accurate central SBP operators and. The results were obtained at the final time t=1.

Table 3: The absolute error in 10-logarithm and convergence rate of the numerical solution $w^{(1)}$, using upwind SBP operators of accuracy orders 3, 7 and 9. An additional SBP operator of accuracy order 9 with optimal boundary closure has been added and is denoted $9(o)$. [6].

n	$\log_{10}\lvert u-w\rvert$	$q_{(3)}$	$\log_{10}\lvert u-w\rvert$	$q_{(7)}$	$\log_{10}\lvert u-w\rvert$	$q_{(9)}$	$\log_{10}\lvert u-w\rvert$	$q_{(9(o))}$
200	-1.6370	-	-3.2293	-	-3.4528	-	-5.2140	-
800	-3.4902	-3.08	-5.6555	-4.03	-6.4500	-4.98	-8.3122	-5.15
1000	-3.8003	-3.20	-6.0437	-4.01	-6.9343	-5.00	-8.7994	-5.03
2000	-4.8135	-3.37	-7.2488	-4.00	-8.4393	-5.00	-10.3084	-5.01
5000	-6.8033	-5.00	-8.8410	-4.00	-10.4293	-5.00	-12.2958	-4.99

Table 4: The absolute error in 10-logarithm and convergence rate of the numerical solution $w^{(1)}$, using central SBP operators of accuracy orders 2, 4 and 6.

n	$\log_{10}\lvert u-w\rvert$	$q_{(2)}$	$\log_{10}\lvert u-w\rvert$	$q_{(4)}$	$\log_{10}\lvert u-w\rvert$	$q_{(6)}$
200	-0.7168	-	-2.3801	-	-3.1263	-
800	-1.9187	-2.00	-4.4384	-3.42	-5.9776	-4.74
1000	-2.1127	-2.00	-4.7531	-3.25	-6.4302	-4.67
2000	-2.7152	-2.00	-5.7085	-3.17	-7.7897	-4.52
5000	-3.5114	-2.00	-6.9372	-3.09	-9.4789	-4.24

4.4 First-order hyperbolic PDE: Advection-diffusion equation

We will end the study of the SBP-P method for a first-order IVP by using it to solve a linear hyperbolic partial differential equation. The problem studied is the advection-diffusion equation which is given on the form

$$\begin{aligned} &u_t = -au_x + \varepsilon u_{xx} + F(x,t), && x_l < x < x_r, && t > 0, \\ &u = g_l, && x = x_l, && t > 0, \\ &u = g_r, && x = x_r, && t > 0, \\ &u = f, && x_l < x < x_r, && t = 0, \end{aligned} \tag{48}$$

where the coefficients were set to $\alpha = 1$ and $\varepsilon = 1$, the boundary conditions were further set to $g_l = g_r = 0$ and the initial condition was defined as a gaussian pulse given by $f = f(x) = \exp\left(-(x/R)^2\right)$, where the width parameter $R = 0.1$. The spatial domain was defined for values of x between $x_l = 0$ and $x_r = 1$, and the time t was integrated from $t = 0$ to $t = 0.5$. A forcing term $F(x,t)$ was designed and added to the problem in order to obtain an analytical solution to compare the numerical results with. The forcing term was designed by the following ansatz of the analytical solution $u(x,t) \equiv \exp\left(-((x-at)/R)^2\right)\exp\left(-\varepsilon t\right)$ and is given as follows:

$$F(x,t) \equiv \varepsilon\left(\frac{2}{R^2} - 1 - \frac{4}{R^2}\left(\frac{x-at}{R}\right)^2\right)\exp\left(-\left(\frac{x-at}{R}\right)^2\right)\exp\left(-\varepsilon t\right). \tag{49}$$

The following continuous energy estimate may be derived for the advection-diffusion problem in (48):

$$2\varepsilon\int_{t_0}^{T}\|u_x\|^2 \mathrm{d}t + \|u(\cdot,T)\|^2 = 0, \tag{50}$$

where the specified values $f = g_l = g_r = F = 0$ has been inserted into (83). The problem in (48) is well-posed since the coefficient $\varepsilon = 1$ and the solution u is defined on both boundaries and at time $t = t_0$.

The projection operators P_x and P_t are created in accordance with Section 2.2 using the linear discrete boundary operator $L_x = (e_0, e_m)$ and initial condition operator $L_t = (e_0)$, respectively. An SBP-P discretization is then obtained by first discretizing the PDE in (48) in space to obtain

$$\begin{aligned} v_t &= -aP_xDP_xv + \varepsilon P_xD_2P_xv + P_x\tilde{\tilde{F}} - \sigma_x(I_m - P_x)v, \quad t > 0, \\ v &= \tilde{\tilde{f}}, \qquad\qquad\qquad\qquad\qquad\qquad\qquad\qquad\qquad\quad t = 0, \end{aligned} \tag{51}$$

where D_2 is a 6th order accurate second derivative SBP operator (see details in [5]), $\tilde{\tilde{F}} \in \mathbb{R}^{m+1}$ is the space-discrete forcing function and $\tilde{\tilde{f}} \in \mathbb{R}^{m+1}$ is the space-discrete initial condition. Here, the boundary terms vanish as they are set to be zero. The full SBP-P discretization is then given, in accordance with Definition 4.1 as:

$$\begin{aligned} (P_tD \otimes I_m)((P_t \otimes I_m)w + ((I_n - P_t) \otimes I_m)\tilde{f}) \\ &= -a(P_t \otimes P_xDP_x)((P_t \otimes I_m)w + ((I_n - P_t) \otimes I_m)\tilde{f}) \\ &+ \varepsilon(P_t \otimes P_xD_2P_x)((P_t \otimes I_m)w + ((I_n - P_t) \otimes I_m)\tilde{f}) \\ &- \sigma_x(P_t \otimes (I_m - Px))((P_t \otimes I_m)w + ((I_n - P_t) \otimes I_m)\tilde{f}) \\ &+ (P_t \otimes P_x)\tilde{F} - \sigma_t((I_n - P_t) \otimes I_m)(w - \tilde{f}), \end{aligned} \tag{52}$$

where $\tilde{f} \in \mathbb{R}^{(m+1)(n+1)}$ is the vector satisfying $(L_t^T \otimes I_m)\tilde{f} = \tilde{\tilde{f}}$, $\tilde{F} \in \mathbb{R}^{(m+1)(n+1)}$ is the fully discrete forcing function and $\sigma_t = \sigma_x = 1$ are the penalty parameters of the projection method.

In order to present the discrete energy estimate, the following notation is introduced:

$$\begin{aligned} \tilde{\tilde{w}} &\equiv (P_t \otimes P_x)w, & \tilde{w} &\equiv (P_t \otimes I_m)w, \\ \tilde{\tilde{w}}_i &\equiv (I_n \otimes e_i^T)\tilde{\tilde{w}}, & \tilde{w}_i &\equiv (I_n \otimes e_i^T)\tilde{w}, \\ (\tilde{\tilde{w}}_i)_x &\equiv (I_n \otimes d_i)\tilde{\tilde{w}}, & (\tilde{w}_i)_x &\equiv (I_n \otimes d_i)\tilde{w}, \\ \tilde{\tilde{w}}^{(j)} &\equiv (e_j^T \otimes I_m)\tilde{\tilde{w}}, & \tilde{w}^{(j)} &\equiv (e_j^T \otimes I_m)\tilde{w}, \end{aligned} \tag{53}$$

where $i = 0, 1, ..., m$ and $j = 0, 1, ..., n$, $\tilde{w}$ and $\tilde{\tilde{w}}$ are the projected solutions. Furthermore, the lower-case i denotes the semi-discrete solution at the spatial grid point x_i. Similarly, the upper-case (j) denotes the semi-discrete solution at time t_j. The operator $(\cdot)_x$ denotes the first derivative in space and is defined as $(w)_x \equiv (I_n \otimes D)w$ for the full discretization w and $(w_i)_x \equiv (I_n \otimes d_i)w$ for a first derivative at the boundaries. Using this notation with a central second derivative SBP operator D_2 (as defined in [7]), the discrete energy estimate is given on the form

$$\begin{aligned} &\text{(central } D_1\text{)}: \qquad 2\varepsilon\|(\tilde{\tilde{w}})_x\|^2_{H_t \otimes H_x} = IC_h + BC_h + PT_h, \\ &\text{(upwind } D_-\text{)}: \qquad 2\varepsilon\|(\tilde{\tilde{w}})_x\|^2_{H_t \otimes H_x} = IC_h + BC_h + PT_h + AD_h, \end{aligned} \tag{54}$$

where the initial condition terms IC_h, the boundary condition terms BC_h, the penalty terms PT_h and the artifical damping term AD_h are given as follows:

$$\begin{aligned} IC_h &= -\|\tilde{w}^{(n)}\|^2_{H_x} + \|\tilde{w}^{(0)}\|^2_{H_x}, \\ BC_h &= -a\left(\|\tilde{\tilde{w}}_m\|^2_{H_t} - \|\tilde{\tilde{w}}_0\|^2_{H_t}\right) + \varepsilon\left(\tilde{\tilde{w}}_m^* H_t(\tilde{\tilde{w}}_m)_x + (\tilde{\tilde{w}}_m)_x^* H_t\tilde{\tilde{w}}_m - \tilde{\tilde{w}}_0^* H_t(\tilde{\tilde{w}}_0)_x - (\tilde{\tilde{w}}_0)_x^* H_t\tilde{\tilde{w}}_0\right), \\ PT_h &= -2\sigma_x\left((I_n \otimes L_x^T)\tilde{w}\right)^*\left(H_t \otimes (L_x^T H_x^{-1} L_x)^{-1}\right)(I_n \otimes L_x^T)\tilde{w} \\ &\quad - 2\sigma_t\left((L_t^T \otimes I_m)w\right)^*\left((L_t^T H_t^{-1} L_t)^{-1} \otimes I_m\right)(L_t^T \otimes I_m)w, \\ AD_h &= \frac{1}{2}\tilde{w}^*(S \otimes H_x)\tilde{w}, \end{aligned} \tag{55}$$

where it should be noted that central SBP operators have been used to discretize in space.

Remark. *The derivations for the continuous and discrete energy estimates are long and similar to the derivation of the energy estimates for an IVP. The interested reader can find the respective derivations in the Appendix (Section 8.1).*

4.4.1 Numerical results

In this section, the results for the advection-diffusion equation is shown. Figure 3 illustrates how the initial gaussian pulse diffuses and propagates to the left over time. A convergence study is presented in Tables 5 and 6, comparing central and upwind SBP operators of different accuracy orders. In order to ensure a small numerical error from the space discretization, a fine grid in space of $m = 400$ grid points has been used in the computations.

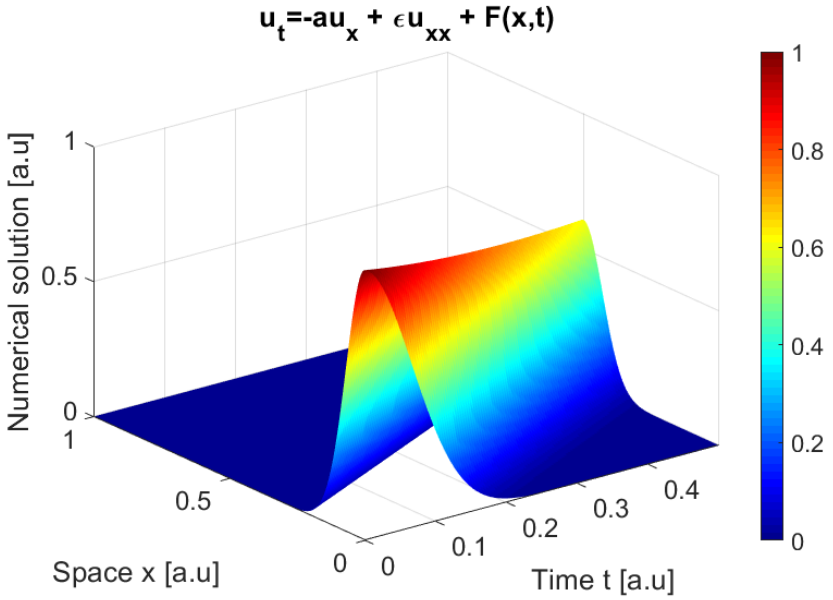

Figure 3: The numerical solution for the advection-diffusion equation, plotted as a surface plot. It is plotted against time for $t = 0$ to $t = 0.5$ seconds and in space between $x = 0$ and $x = 1$.

Table 5: 10-logarithm of l^2-norm of the errors and convergence rates for the numerical solution at $t = 0.5$ using central SBP operators. A 6th order central SBP operator was used on a spatial discretization of 400 grid points.

n	$\log_{10} l^2(u-w)$	$q_{(2)}$	$\log_{10} l^2(u-w)$	$q_{(4)}$	$\log_{10} l^2(u-w)$	$q_{(6)}$
30	-3.0429		-3.7961		-4.1650	
70	-3.5806	-1.46	-4.7365	-2.56	-5.4537	-3.50
100	-3.8232	-1.57	-5.1617	-2.74	-6.0303	-3.72

Table 6: 10-logarithm of l^2-norm of the errors and convergence rates for the numerical solution at $t = 0.5$ using upwind SBP operators. A 6th order central SBP operator was used on a spatial discretization of 400 grid points.

n	$\log_{10} l^2(u-w)$	$q_{(3)}$	$\log_{10} l^2(u-w)$	$q_{(7)}$	$\log_{10} l^2(u-w)$	$q_{(9)}$
30	-3.5915		-4.1584		-4.3651	-
70	-4.2903	-1.90	-5.4478	-3.50	-5.9952	-4.43
100	-4.5826	-1.89	-6.0254	-3.73	-6.7210	-4.69

5 SBP in time: Second derivative

In this section, the SBP-P method in time is extended to IVPs on second-order form. A linear second-order IVP can be written on the form

$$\begin{aligned} Av_{tt} + Bv_t + Cv &= F_c(t), \quad t > 0, \\ L_c^T u &= f_c, \qquad\qquad t = 0, \end{aligned} \tag{56}$$

where $v = v(t) \in \mathbb{R}^{m+1}$ is the time-dependent exact solution. The coefficients A, B and C are matrices defined in the matrix space $\mathbb{R}^{(m+1)\times(m+1)}$, resulting in a more general problem which may come from a space discretization using i.e. a finite difference or finite element method. The initial condition vector $f_c \in \mathbb{R}^{2(m+1)}$ is on the form $f_c = (f_1, f_2)^T$ and L_c is the discrete linear initial condition operator $L_c \in \mathbb{R}^{(m+1)\times 2(m+1)}$. Finally $F_c(t) \in \mathbb{R}^{m+1}$ is a forcing term.

Definition 5.1. Let D be a first derivative summation by parts operator based on a symmetric positive definite matrix H. Let further P_t be a projection operator created as in equation (15) and $L_t \in \mathbb{R}^{n+1\times 2}$ a discrete linear initial condition operator satisfying $(L_t^T \otimes I_m)w = f$, for $f \in \mathbb{R}^{2(m+1)}$. Then a SBP-P discretization of the IVP in equation (56) is defined as:

$$\begin{aligned}(P_t^T D^T H \otimes I_m)\Big((DD \otimes A)\big((P_t \otimes I_m)w + ((I_n - P_t) \otimes I_m)\tilde{f}\big) \\ +(D \otimes B)\big((P_t \otimes I_m)w + ((I_n - P_t) \otimes I_m)\tilde{f}\big)\Big) \\ +(I_n \otimes C)\big((P_t \otimes I_m)w + ((I_n - P_t) \otimes I_m)\tilde{f}\big)\Big) \\ = (P_t^T D^T H \otimes I_m)F - \frac{\sigma_t}{k}\big(H(I_n - P_t) \otimes I_m\big)(w - \tilde{f}), \quad \sigma_t > 0,\end{aligned} \tag{57}$$

where $w \in \mathbb{R}^{(m+1)(n+1)}$ is the fully-discrete numerical solution, $I_n \in \mathbb{R}^{(n+1)\times(n+1)}$ and $I_m \in \mathbb{R}^{(m+1)\times(m+1)}$ are identity matrices and k is the time-step. Finally $F \in \mathbb{R}^{(m+1)(n+1)}$ is the fully discrete forcing term and $\tilde{f} \in \mathbb{R}^{(m+1)(n+1)}$ is a discrete vector satisfying $(L_t^T \otimes I_m)\tilde{f} = f$.

Remark. *The outer projection $(P_t \otimes I_m)$ needs to be replaced by a preconditioning term $(P_t^T D^T H_t \otimes I_m)$, when extending the SBP-P method to a second-order IVP. This is done in order to prove the stability of the numerical method. First-order IVPs can be solved without a preconditioner as the symmetric property of the projection operator $H_t P_t = P_t^T H_t$ holds. When extending to a second-order IVP, the discrete problem is multiplied by $((D \otimes I_m)w)^* H_t$ which leads to $D^T H_t P_t \neq P_t^T D^T H_t$. The preconditioner fixes this problem, and the discrete problem is multiplied by w^* to achieve a discrete energy estimate.*

5.1 Stability of discretization

For the SBP-P discretization in Definition 5.1 to be stable, it is required that D is a first derivative SBP operator. In addition, the IVP in (56) needs to be well-posed. This is fulfilled in parts by setting the correct number of initial conditions (two for a second-order IVP). The coefficients A, B and C also needs to satisfy certain criteria. These criteria is investigated with the continuous energy method in Section 5.1.1 and the results will be used in Section 5.1.2 to derive a discrete energy estimate for the SBP-P discretization.

5.1.1 Continuous energy estimate

The energy method is used to derive a continuous energy estimate for the second-order IVP in (56). The procedure is similar to that described in Section 4.1.1 and we start off by multiplying the IVP in (56) by the complex conjugate transpose v_t^* from the left to get

$$\langle v_t, Av_{tt} + (v_t, Bv_t\rangle + \langle v_t, Cv\rangle = 0. \tag{58}$$

Adding the complex conjugate transpose of the results in (58) to itself leads to

$$\langle v_t, Av_{tt}\rangle + \langle v_t, Bv_t\rangle + \langle v_t, Cv\rangle + \langle v_{tt}, A^* v_t\rangle + \langle v_t, B^* v_t\rangle + \langle v, C^* v_t\rangle = 0. \tag{59}$$

By introducing the restrictions $A = A^*$, $C = C^*$ and making use of the product differentiation rule, the following energy rate is obtained:

$$\frac{d}{dt}\left(\|v_t\|_A^2 + \|v\|_C^2\right) + \|v_t\|_{B+B^*}^2 = 0. \tag{60}$$

From the energy rate it may be seen that no energy growth is possible if the coefficient matrices satisfy $A = A^* > 0$, $B + B^* \geq 0$ and $C = C^* \geq 0$. Integrating the energy rate expression over time then leads to the continuous energy estimate:

$$\begin{aligned} \|v_t(T)\|_A^2 + \|v(T)\|_C^2 + \int_{t_0}^{T} \|v_t\|_{B+B^*}^2 &= \|v_t(t_0)\|_A^2 + \|v(t_0)\|_C^2 \\ &= \|f_1\|_A^2 + \|f_2\|_C^2 \\ &= 0, \end{aligned} \tag{61}$$

which shows that the IVP in (56) is well-posed if the initial data is set for $v(t_0)$ and $v_t(t_0)$ and the coefficient matrices fulfill $A = A^* > 0$, $C = C^* \geq 0$ and $B + B^* \geq 0$.

5.1.2 Discrete energy estimate

Knowing that the underlying IVP is well-posed, it remains to show that the numerical solution w is bounded in order to guarantee stability of the SBP-P method. This can be proved using the discrete energy method to derive a discrete energy estimate. The SBP-P discretization in Definition 5.1 is therefore multiplied by w^* from the left and known data are set to zero, in order to get

$$\begin{aligned} w^*(P_t^T D^T HDDP_t \otimes A)w + w^*(P_t^T D^T HDP_t \otimes B)w \\ + w^*(P_t^T D^T HP_t \otimes C)w = -\frac{\sigma_t}{k} w^*\big(H(I_n - P_t) \otimes I_m\big)w. \end{aligned} \tag{62}$$

Adding the complex conjugate transpose of 62 to itself and using the criteria specified for the coefficient matrices in Section 5.1.1 leads to

$$\begin{aligned} & w^*(P_t^T D^T \otimes I_m)\left([HD + D^T H] \otimes A\right)(DP_t \otimes I_m)w \\ & + w^*(P_t^T D^T \otimes I_m)\left(H \otimes [B + B^*]\right)(DP_t \otimes I_m)w \\ & + w^*(P_t^T \otimes I_m)\left([HD + D^T H] \otimes C\right)(P_t \otimes I_m)w \\ & = -\frac{2\sigma_t}{k}\left((L_t^T \otimes I_m)w\right)^*\left((L_t^T H^{-1} L_t)^{-1} \otimes I_m\right)\left((L_t^T \otimes I_m)w\right). \end{aligned} \tag{63}$$

Now, using the results from Lemma 4.1 and 4.2 we may rewrite the expression in equation (63) into the following discrete energy estimate:

$$\begin{aligned} &\text{(central } D_1\text{)}: \quad \|\tilde{w}_t^{(n)}\|_A^2 + \|\tilde{w}_t\|_{H\otimes(B+B^*)}^2 + \|\tilde{w}^{(n)}\|_C^2 = IC_h + PT_h, \\ &\text{(upwind } D_-\text{)}: \quad \|\tilde{w}_t^{(n)}\|_A^2 + \|\tilde{w}_t\|_{H\otimes(B+B^*)}^2 + \|\tilde{w}^{(n)}\|_C^2 = IC_h + AD_h + PT_h, \end{aligned} \tag{64}$$

where $\tilde{w} = (P_t \otimes I_m)w$ denotes the projected solution and $\tilde{w}_t = (DP_t \otimes I_m)w$ the first derivative of the projected solution. Additionally, IC_h holds the discrete initial condition terms, AD_h the discrete artificial dissipation terms and PT_h the penalty terms and are given as follows:

$$\begin{aligned} IC_h &\equiv \|\tilde{w}_t^{(0)}\|_A^2 + \|\tilde{w}^{(0)}\|_C^2, \\ AD_h &\equiv \frac{1}{2}\tilde{w}_t^*(S \otimes A)\tilde{w}_t + \frac{1}{2}\tilde{w}^*\left(S \otimes C\right)\tilde{w}, \\ PT_h &\equiv -\frac{2\sigma_t}{k}\left((L_t^T \otimes I_m)w\right)^*\left((L_t^T H^{-1} L_t)^{-1} \otimes I_m\right)\left((L_t^T \otimes I_m)w\right). \end{aligned} \tag{65}$$

The discrete energy estimate in (64) mimics the continuous energy estimate, with additional terms which provide damping.

Remark. *The current SBP-P implementation defined as in Definition 5.1 requires the use of first derivative SBP-operators with a diagonal norm (as described in Section 2.1) in order to satisfy the criteria for stability. A second derivative approximation in time is thus obtained by the combination of central $D = D_1$ operators or upwind $D = D_-$ operators as $D_2 \equiv DD$, respectively.*

5.2 A second-order ODE

The scalar coefficient case of the more general second-order IVP in (56) is studied in this section. This problem is stated as follows:

$$\begin{aligned} &u_{tt} + \alpha u_t + \beta u = F_c(t), && t > 0, \\ &u = f_1, && t = 0, \\ &u_t = f_2, && t = 0, \end{aligned} \tag{66}$$

where $u = u(t) \in \mathbb{R}$ is the exact solution and the coefficients are scalar parameters $\alpha \in \mathbb{R}$ and $\beta \in \mathbb{R}$. The time was integrated from $t = 0$ to $t = 4$ and the initial conditions were set to $u(0) = 1$ and $u_t(0) = 0$, respectively. The forcing function was further set to $F(t) = \tilde{C} \sin(\kappa t)$, where $\tilde{C} = \alpha\kappa/4$ and $\kappa = 9\pi/2$.

Both the continuous and discrete energy estimates are then analogous with those derived for (56) in (61) and (64), by inserting $m = 0$. Similarly, the SBP-P implementation is given as in Definition 5.1 (with insertion of $m = 0$).

5.2.1 Numerical results (non-stiff scalar IVP)

In this section the convergence results are presented from using the SBP-P method to numerically solve the IVP in (66). The scalar coefficients were set to $\alpha = \beta = 1$ and an analytical solution to this problem is given as

$$\begin{aligned} u(t) &= (c_1 \cos(\mu t) + c_2 \sin(\mu t))\, e^{-\frac{\alpha}{2}t} + c_3 \sin(\kappa t) + c_4 \cos(\kappa t), \\ c_1 &= u(0) - c_4, \\ c_2 &= \frac{u_t(0) + \frac{\alpha}{2}u(0) - \frac{\alpha}{2}c_4 - \kappa c_3}{\mu}, \\ c_3 &= \frac{\tilde{C}(\beta - \kappa^2)}{\alpha^2\kappa^2 + (\beta - \kappa^2)^2}, \\ c_4 &= \frac{c_3(\beta - \kappa^2) - \tilde{C}}{\alpha\kappa}, \end{aligned} \tag{67}$$

where $\mu = \mathrm{Im}\left(\frac{1}{2}\sqrt{\alpha^2 - 4\beta}\right)$.

In Figure 4, the absolute error is shown for the numerical solutions with different number of grid points n in time. It may be seen that the convergence rate slows down and changes sign at approximately $n = 2000$ for each of the used SBP operators. These convergence results may be compared with the condition numbers of the respective matrices in the SBP-P discretization (see Figure 5).

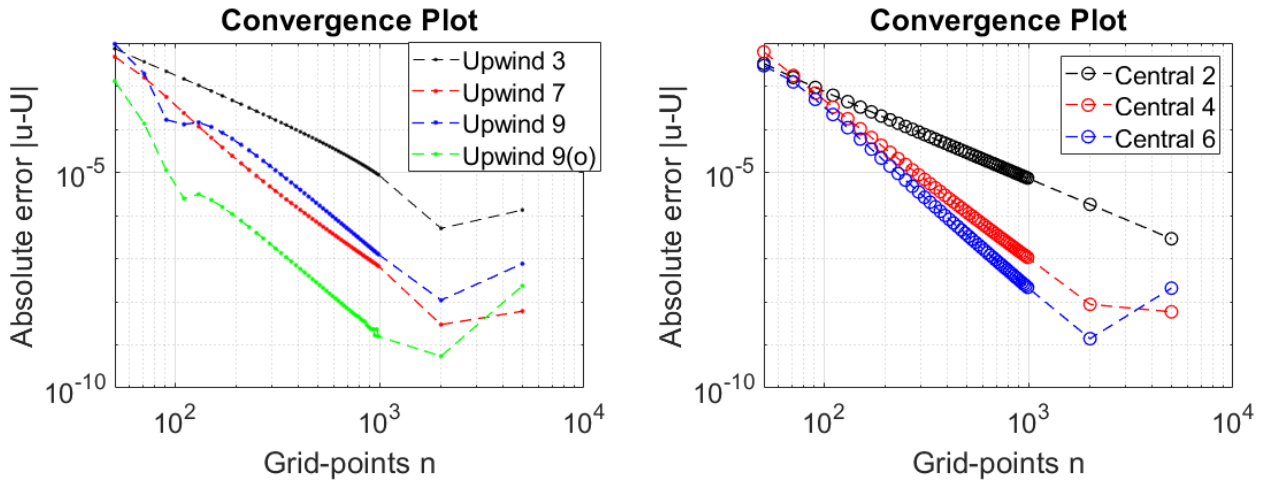

(a) (b)

Figure 4: The absolute error $|u - w|$ at the final time $t = 4$ seconds is plotted against the number of grid points n. (a) shows the results using upwind- and (b) using central SBP operators.

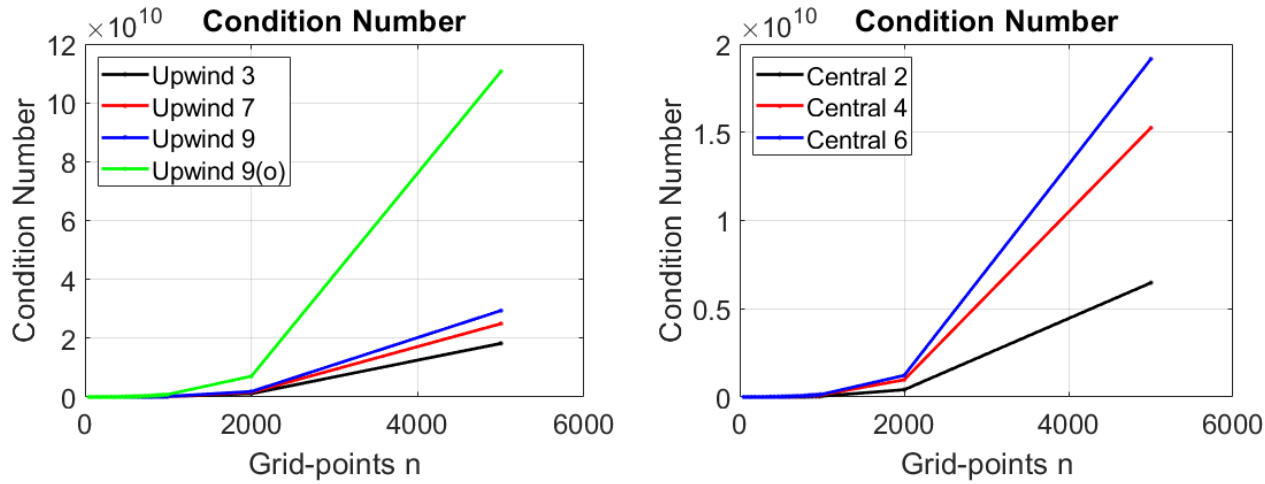

(a) (b)

Figure 5: The condition number (2-norm) of the equation system plotted against the number of grid points n. (a) shows the results using upwind- and (b) using central SBP operators.

Remark. *The condition number of the matrices in the second-order SBP-P implementations are increasing nonlinearly and should be compared with the corresponding results from first-order implementations in Figure 2. For the first-order IVP, the condition number grows linearly with the number of grid points. It may further be seen that the condition number increases with the accuracy-order of the used SBP operator. This nonlinear growth is believed to be the reason to why the SBP-P method stagnates, using the "\"-operator in* `MATLAB`*. A lower error could be obtained using higher arithmetic precision.*

In Tables 7 and 8 we present convergence results using 2nd, 4th and 6th order accurate central- and 3rd, 7th and 9th order accurate upwind SBP operators, respectively. In Table 8 an additional 9th order accurate upwind SBP operator has been studied. This operator has an optimal boundary closure and is described in detail in [6].

Table 7: Shows the 10-logarithm of the absolute error of the numerical solution w at the final time $t = 4$ seconds. The computations were made using central SBP operators of orders 2, 4 and 6.

n	$\log_{10}\|u-w\|$	$q_{(2)}$	$\log_{10}\|u-w\|$	$q_{(4)}$	$\log_{10}\|u-w\|$	$q_{(6)}$
51	-2.4752	-	-2.2058	-	-2.5254	-
201	-3.7394	-2.12	-4.4558	-3.78	-4.7649	-3.76
501	-4.5384	-2.01	-5.9218	-3.70	-6.4471	-4.24
801	-4.9470	-2.00	-6.6491	-3.57	-7.2880	-4.13
1001	-5.1409	-2.00	-6.9875	-3.50	-7.6858	-4.11

Table 8: Shows the 10-logarithm of the absolute error of the numerical solution w at the final time $t = 4$ seconds. The computations were made using upwind SBP operators of orders 3, 7 and 9. An additional SBP operator of order 9 with optimal boundary closure was also added and is denoted $9(o)$.

n	$\log_{10}\|u-w\|$	$q_{(3)}$	$\log_{10}\|u-w\|$	$q_{(7)}$	$\log_{10}\|u-w\|$	$q_{(9)}$	$\log_{10}\|u-w\|$	$q_{(9(o))}$
51	-2.1304	-	-2.3188	-	-2.0216	-	-2.8886	-
201	-3.3748	-2.09	-4.7060	-4.01	-4.2908	-3.81	-6.0454	-5.30
501	-4.2603	-2.23	-6.1726	-3.70	-5.7380	-3.65	-7.5819	-3.87
801	-4.7814	-2.56	-6.8656	-3.40	-6.5376	-3.92	-8.3944	-3.99
1001	-5.0711	-2.99	-7.1862	-3.31	-6.9205	-3.96	-8.7357	-3.53

5.2.2 Numerical results (stiff scalar IVP)

In this section, the same study is made as in Section 5.2.1 but with a different coefficient for $\alpha \in \mathbb{R}$ in the IVP of (56), which is here set to $\alpha = 10^7$. This choice of parameter leads to a solution with a rapid damping event in the beginning. The analytical solution is in this case given by

$$\begin{aligned} u(t) &= c_1 e^{r_1 t} + c_2 e^{r_2 t} + c_3 \sin(\kappa t) + c_4 \cos(\kappa t), \\ c_1 &= u(0) - c_2 - c_4, \\ c_2 &= \frac{u_t(0) + r_1(c_4 - u(0))}{r_2 - r_1}, \\ c_3 &= \frac{C(\beta - \kappa^2)}{\alpha^2\kappa^2 + (\beta - \kappa^2)^2}, \\ c_4 &= \frac{c_3(\beta - \kappa^2) - C}{\alpha\kappa}, \end{aligned} \tag{68}$$

where $r_{1,2} = -\frac{\alpha}{2} \pm \frac{1}{2}\sqrt{\alpha^2 - 4\beta}$.

The results from the convergence study are presented in Table 9 and 10 for simulations with the SBP-P method using 2nd, 4th and 6th order accurate central- and 3rd, 7th and 9th order accurate upwind SBP operators, respectively. Comparing these results, it is seen that a lower absolute error was obtained when using central SBP operators.

Table 9: Shows the 10-logarithm of the absolute error of the numerical solution $u(t)$ at the final time $t = 4$. The computations were made using central SBP operators of orders 2, 4 and 6.

n	$\log_{10}\|u-w\|$	$q_{(2)}$	$\log_{10}\|u-w\|$	$q_{(4)}$	$\log_{10}\|u-w\|$	$q_{(6)}$
51	-5.7543	-	-5.7482	-	-5.7051	-
201	-6.2916	-0.90	-6.4277	-1.14	-6.4883	-1.32
501	-6.6887	-1.00	-6.8375	-1.03	-6.8891	-1.01
801	-6.8932	-1.00	-7.0429	-1.01	-7.0934	-1.00
1001	-6.9903	-1.00	-7.1407	-1.01	-7.1896	-0.99

Table 10: Shows the 10-logarithm of the absolute error of the numerical solution $u(t)$ at the final time $t = 4$. The computations were made using upwind SBP operators of orders 3, 7 and 9. An additional SBP operator of order 9 with optimal boundary closure was also added and is denoted $9(o)$.

n	$\log_{10}\|u-w\|$	$q_{(3)}$	$\log_{10}\|u-w\|$	$q_{(7)}$	$\log_{10}\|u-w\|$	$q_{(9)}$	$\log_{10}\|u-w\|$	$q_{(9(o))}$
51	-1.4388	-	-2.2082	-	-1.9784	-	-3.2985	-
201	-3.9352	-4.19	-4.0616	-3.11	-4.2116	-3.75	-6.3324	-5.09
501	-4.3384	-1.02	-5.5752	-3.82	-6.3663	-5.43	-7.2266	-2.25
801	-4.7163	-1.85	-6.3171	-3.64	-6.9733	-2.98	-7.4120	-0.91
1001	-4.9029	-1.93	-6.6300	-3.23	-7.1189	-1.50	-7.5098	-1.01

The nonlinear growth of the condition number is similar to the non-stiff case, as may be seen in Figure 6. The magnitude of the condition number is however lower, as compared to the non-stiff IVP studied in the previous Section 5.2.1. This suggests that increasing α from $\alpha = 1$ to $\alpha = 10^7$ leads to a more well-conditioned equation system.

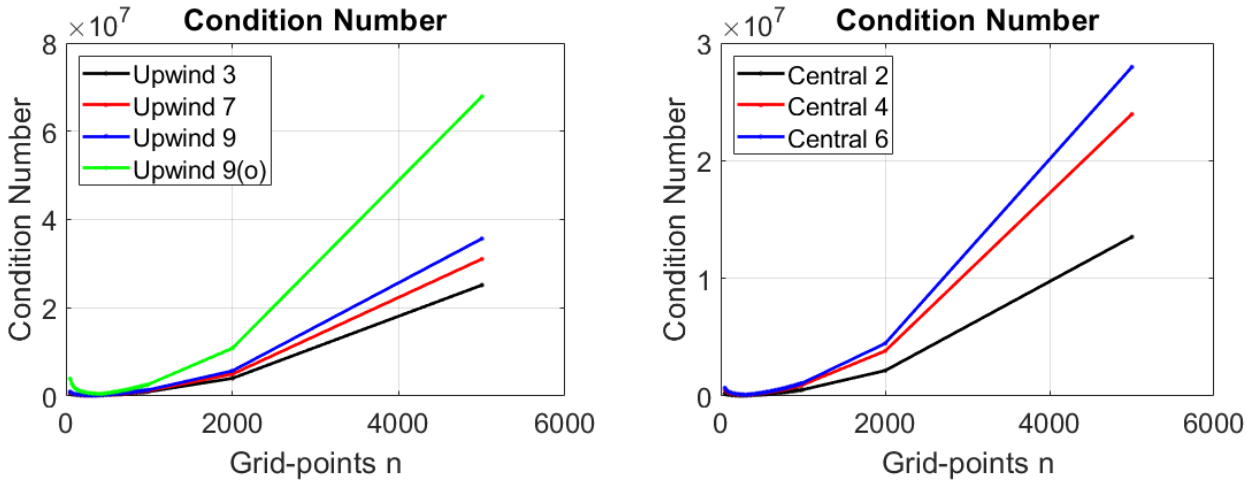

(a) (b)

Figure 6: The condition number (2-norm) of the system of equations plotted against the number of grid points n. (a) shows the results using upwind- and (b) using central SBP operators.

A performance study is presented in Figure 7, where the stiff second-order IVP in (66) is solved using the SBP-P method and with the explicit fourth-order accurate Runge-Kutta method (RK4), respectively. A 9th order accurate upwind SBP operator was used in the SBP-P discretization. For the implementation with RK4, the IVP in (66) was rewritten as a system of two first-order IVP and time-integrated using $(2, 3, 4, 5, 10) \cdot 10^7$ steps. It should be noted that a smaller absolute error could be reached using the SBP-P method at a fraction of the time, as compared to the RK4 method for this specific problem. This shows that there exist problems where it is beneficial to use the SBP-P method over the popular RK4 method.

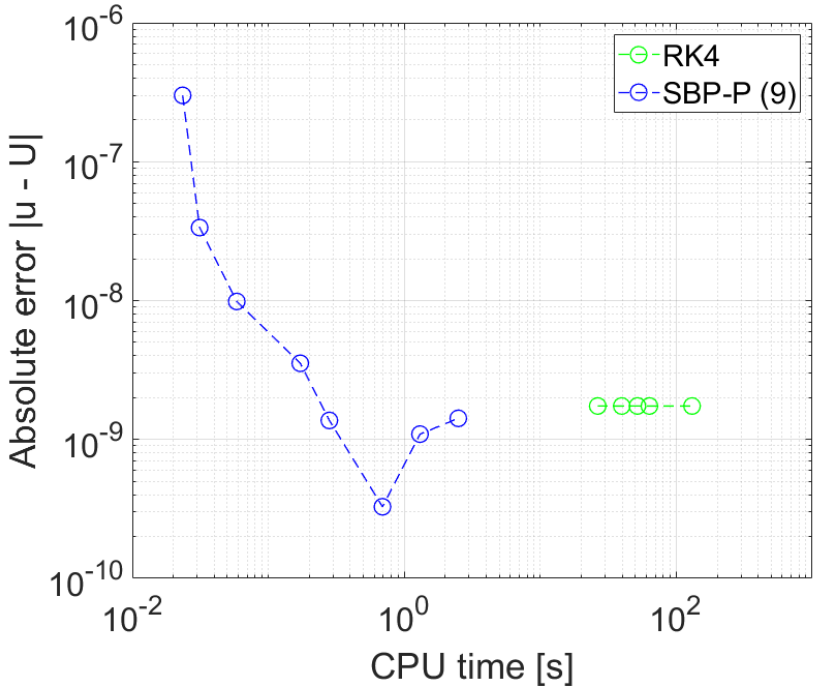

Figure 7: The absolute error plotted against the CPU time. The computations were made using the SBP-P method with a 9th order accurate upwind SBP operator and with the explicit RK4 method.

Remark. *It should be noted that the IVP in (66) is stiff for the choice of parameters $\alpha = 10^7$ and $\beta = 1$. As RK4 is an explicit finite difference method, it yields an unstable solution to this problem if the time-domain is insufficiently resolved. RK4 was found to be stable for grid points $n \geq 1.5 \cdot 10^7$. This is why the lowest integer multiple used in the performance study was set to $n = 2 \cdot 10^7$ grid points in time.*

5.3 Second-order parabolic PDE: Dynamic beam equation

In this section, a stable SBP-P method is presented for solving the dynamic beam equation on second and first order form. The dynamic beam equation is given on the following form:

$$\begin{aligned} &u_{tt} = -\alpha u_{xxxx}, && x_l < x < x_r, && t > 0, \\ &L_l^T u = g_l, && x = x_l, && t > 0, \\ &L_r^T u = g_r, && x = x_r, && t > 0, \\ &L_{ic}^T u = f, && x_l < x < x_r, && t = 0, \end{aligned} \tag{69}$$

where the coefficient α is set to $\alpha = 1$, the final time is set to $t = 0.5$ and the boundaries are set to $x_l = -1$ and $x_r = 1$, respectively. The linear boundary operators $L_l \in \mathbb{R}^{1\times 2}$ and $L_r \in \mathbb{R}^{1\times 2}$ are both set to $(1, \frac{d}{dx})$ which together with boundary parameters $g_l = g_r = 0$ leads to clamped boundary conditions for the beam. Similarly, the linear operator $L_{ic} \in \mathbb{R}^{1\times 2}$ is set to $L_{ic} = (1, \frac{d}{dt})$ and the initial condition function $f = (f_1, f_2)^T \in \mathbb{R}^2$, where the initial velocity is set to $f_2 = 0$ and with an initial deflection $f_1 = f_1(x)$ given by a shifted gaussian on the form

$$f_1(x) \equiv \exp\left(-\frac{(x - x_*)^2}{R}\right), \tag{70}$$

where $x_* = 0.1$ determines the shift of the gaussian from the centerpoint and $R = 0.1$ the width of the gaussian.

The following continuous energy estimate may be derived for the dynamic beam equation on the form in (69):

$$\begin{aligned}\|u_t(\cdot,T)\|^2+\alpha\|u_{xx}(\cdot,T)\|^2 =&\|u_t(\cdot,t_0)\|^2+\alpha\|u_{xx}(\cdot,t_0)\|^2\\ &+2\alpha\int_{t_0}^{T}(u^*_{tx}(x_r,t)u_{xx}(x_r,t)-u^*_t(x_r,t)u_{xxx}(x_r,t))\mathrm{d}t\\ &-2\alpha\int_{t_0}^{T}(u^*_{tx}(x_l,t)u_{xx}(x_l,t)-u^*_t(x_l,t)u_{xxx}(x_l,t))\mathrm{d}t.\end{aligned}\tag{71}$$

Inserting the specified values $f=g_l=g_r=0$ for the solution at time $t=t_0$ and at the boundaries leads to the simplified expression of (71):

$$\|u_t(\cdot,T)\|^2+\alpha\|u_{xx}(\cdot,T)\|^2=0,\tag{72}$$

which yields a well-posed problem because u and u_t are specified at time $t=t_0=0$, the parameter $\alpha=1$ is positive and both u and u_x are specified at both boundaries.

The dynamic beam equation is discretized in space using the SBP-P method (as in Section 4.4) with 6th order accurate central SBP operators (see [3, 5] for details). The resulting semi-discrete second-order IVP is then given on the form

$$\begin{aligned}&v_{tt}=\alpha\left(P_xD_4P_x-\sigma_x(I_m-P_x)\right)v\equiv Mv, && t>0,\\ &(L_{ic}^T\otimes I_m)v=\tilde{\tilde{f}}, && t=0,\end{aligned}\tag{73}$$

where $\sigma_x=1$ and $M\in\mathbb{R}^{(m+1)\times(m+1)}$. The boundary conditions are homogeneous and are therefore not explicitly shown to reduce the number of terms in the expression. Here the initial condition is given as $\tilde{\tilde{f}}\in\mathbb{R}^{2(m+1)}$ and D_4 denotes a 6th order accurate central fourth derivative SBP operator (see definition in [3]). The full SBP-P discretization is then given, in accordance with Definition 5.1, as follows:

$$\begin{aligned}(P_t^TD_{(t)}^TH_tD_{(t)}D_{(t)}\otimes I_m)&\left((P_t\otimes I_m)w+((I_n-P_t)\otimes I_m)\tilde{f}\right)\\ &=(P_t^TD_{(t)}^TH_t\otimes M)\left((P_t\otimes I_m)w+((I_n-P_t)\otimes I_m)\tilde{f}\right)\\ &-\frac{\sigma_t}{k}((I_n-P_t)\otimes I_m)(w-\tilde{f}),\end{aligned}\tag{74}$$

where $\sigma_t=k^{-2}$ and the discrete vector $\tilde{f}\in\mathbb{R}^{(n+1)(m+1)}$ satisfies the equation $(L_t^T\otimes I_m)\tilde{f}=\tilde{\tilde{f}}$. In this section, SBP operators in time are denoted $D_{(t)}$ for clarity and the discrete linear initial condition operator $L_t\in\mathbb{R}^{(n+1)\times 2}$ is created as $L_t\equiv\left(e_0,(e_0^TD_{(t)})^T\right)$. The discretization in (74) yields the following discrete energy estimate:

$$\begin{aligned}&\text{(central } D_1):\quad &&\|\tilde{\tilde{w}}_t^{(n)}\|^2_{H_x}+\alpha\|\tilde{\tilde{w}}^{(n)}\|^2_N=\|\tilde{\tilde{w}}_t^{(0)}\|^2_{H_x}+\alpha\|\tilde{\tilde{w}}^{(0)}\|^2_N+BC_h+PT_h,\\ &\text{(upwind } D_-):\quad &&\|\tilde{\tilde{w}}_t^{(n)}\|^2_{H_x}+\alpha\|\tilde{\tilde{w}}^{(n)}\|^2_N=\|\tilde{\tilde{w}}_t^{(0)}\|^2_{H_x}+\alpha\|\tilde{\tilde{w}}^{(0)}\|^2_N+BC_h+AD_h+PT_h,\end{aligned}\tag{75}$$

where BC_h, AD_h and PT_h are given by

$$\begin{aligned}BC_h=&\,2\alpha\left(\left(D_{(t)}\tilde{\tilde{w}}_m\right)_x^*H_t\left(\tilde{\tilde{w}}_m\right)_{xx}-\left(D_{(t)}\tilde{\tilde{w}}_m\right)^*H_t\left(\tilde{\tilde{w}}_m\right)_{xxx}\right)\\ &-2\alpha\left(\left(D_{(t)}\tilde{\tilde{w}}_0\right)_x^*H_t\left(\tilde{\tilde{w}}_0\right)_{xx}-\left(D_{(t)}\tilde{\tilde{w}}_0\right)^*H_t\left(\tilde{\tilde{w}}_0\right)_{xxx}\right),\\ AD_h=&\,\frac{1}{2}\tilde{\tilde{w}}_t^*\left(S\otimes H_x\right)\tilde{\tilde{w}}_t+\frac{1}{2}\tilde{\tilde{w}}^*\left(S\otimes N\right)\tilde{\tilde{w}}\\ &+\sigma_x\left((I_n\otimes L_x^T)\tilde{w}\right)^*\left(S\otimes\left(L_x^TH_x^{-1}L_x\right)^{-1}\right)(I_n\otimes L_x^T)\tilde{w},\\ PT_h=&-\sigma_x\left\{\left(L_x^T\tilde{w}^{(n)}\right)^*\left(L_x^TH_x^{-1}L_x\right)^{-1}L_x^T\tilde{w}^{(n)}-\left(L_x^T\tilde{w}^{(0)}\right)^*\left(L_x^TH_x^{-1}L_x\right)^{-1}L_x^T\tilde{w}^{(0)}\right\}\\ &-\frac{\sigma_t}{k}\left((L_t^T\otimes I_m)w\right)^*\left((L_t^TH_t^{-1}L_t)^{-1}\otimes H_x\right)(L_t^T\otimes I_m)w,\end{aligned}\tag{76}$$

where it should be noted that central SBP operators have been used to discretize in space and the matrix N fulfills $N = N^T \geq 0$. The notation used in the discrete energy estimates is explained in (53). Additionally, the notation for a discrete second derivative at the boundary points is given on the form $(w_i)_{xx} \equiv (I_n \otimes d_{2:i})w$, where $d_{2:i} = e_i^T D_2$. Similarly a discrete third derivative at the boundary points is given as $(w_i)_{xxx} \equiv (I_n \otimes d_{3:i})w$, where $d_{3:i} = e_i^T D_3$.

Remark. *The derivations for the continuous and discrete energy estimates are long and similar to the derivation of the energy estimates for an IVP. The interested reader may find the respective derivations in the Appendix (Section 8.2).*

5.3.1 Dynamic beam equation on first-order form

In order to compare the second-order and first-order implementation fairly, the semi-discrete dynamic beam equation in (73) was rewritten as a system of first-order IVP using the substitution $v_t = \bar{v}$ as

$$\begin{aligned} \bar{\bar{v}}_t &= \begin{bmatrix} 0 & I_m \\ M & 0 \end{bmatrix} \bar{\bar{v}} \equiv \tilde{Q}\bar{\bar{v}}, \\ \bar{\bar{v}} &= (v, \bar{v})^T, \\ (L_{ic}^T \otimes I_m)\bar{\bar{v}} &= \tilde{\bar{f}}. \end{aligned} \tag{77}$$

The first-order IVP of equation (77) was then discretized using the SBP-P method to obtain:

$$\begin{aligned} \left[(P_t D_{(t)} \otimes I_m) \otimes I_2\right] \left([(P_t \otimes I_m) \otimes I_2]\bar{\bar{w}} + [((I_n - P_t) \otimes I_m) \otimes I_2]\bar{f}\right) \\ = (P_t \otimes \tilde{Q})\bar{\bar{w}} \\ - \sigma_t[((I_n - P_t) \otimes I_m) \otimes I_2](\bar{\bar{w}} - \bar{f}), \end{aligned} \tag{78}$$

where $\bar{f} \in \mathbb{R}^{2(n+1)(m+1)}$ is the discrete vector satisfying $[(e_0^T \otimes I_m) \otimes I_2]\bar{f} = \tilde{\bar{f}}$.

5.3.2 Numerical results

The dynamic beam equation in (69) was solved using 201 grid points in space and with a 6th order-accurate central SBP operator for approximating the fourth derivative. The resulting second-order IVP in (73) was rewritten on first-order form as shown in (77) and time-integrated with the explicit RK4 method. The time-integration was done using two different time-step restrictions, in order to obtain a solution to compare the discretizations in (74) and (78) with. These restrictions were $k_1 < 0.1h^2$ and $k_2 < 0.5h^3$. The resulting numerical solution had an l^2-error of $l^2(u^{(k_2)} - u^{(k_1)}) = 3.4596 \times 10^{-6}$. This suggests that the RK4 solution (following the quadratic time-restriction) is accurate to five decimal places. Another solution was also obtained with RK4, using the time-step k_2 for $m = 401$ grid points in space. A comparison between the two RK4 solutions is shown in Figure 8. This plot shows that the space is nicely resolved using 201 grid points in space.

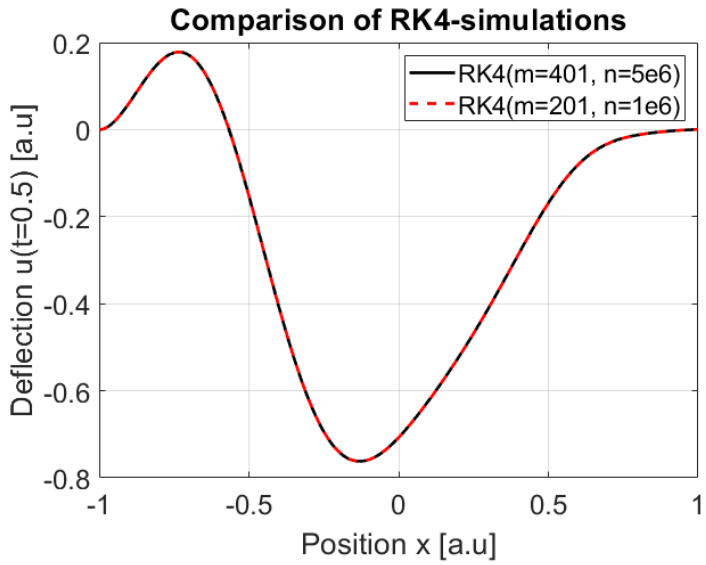

Figure 8: Comparison between two numerical solutions of the dynamic beam equations at $t = 0.5$ seconds. The computations were done using RK4 with 401 grid points in space and $5 \cdot 10^6$ points in time as well as with 201 grid points in space and 10^6 points in time.

Figure 9 shows a comparison between the SBP-P method implemented directly to solve the second-order IVP in (74) (direct) and the first-order IVP in (78) (system). The figure shows the obtained l^2-error given for a certain matrix size. The matrix size is here taken to be its number of rows.

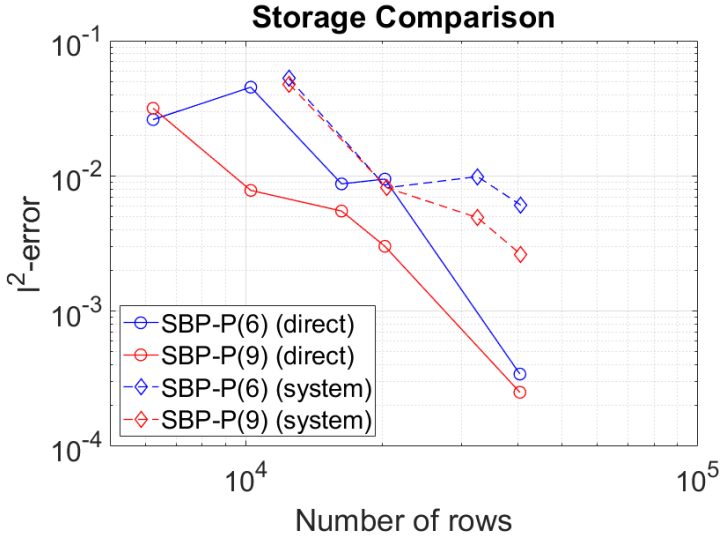

Figure 9: l^2-error plotted against the number of rows in the solved system, using SBP-P to solve equation (73) as a second-order IVP (direct) and as a system of first-order IVP (system) in time.

Figure 10 shows a comparison between the obtained solutions to (69) using a 6th order accurate central SBP operator (left) and a 7th order accurate upwind SBP operator (right) with 201 spatial grid points. The time domain is underresolved with 81 grid points in time. This leads to small spurious oscillations in the solution for a central SBP operator. These oscillations are heavily reduced (or eliminated), when using upwind SBP operators due to the additional energy dissipation it introduces to the problem. This specific comparison illustrates the strength of upwind SBP operators and exemplifies its usability for stiff problems.

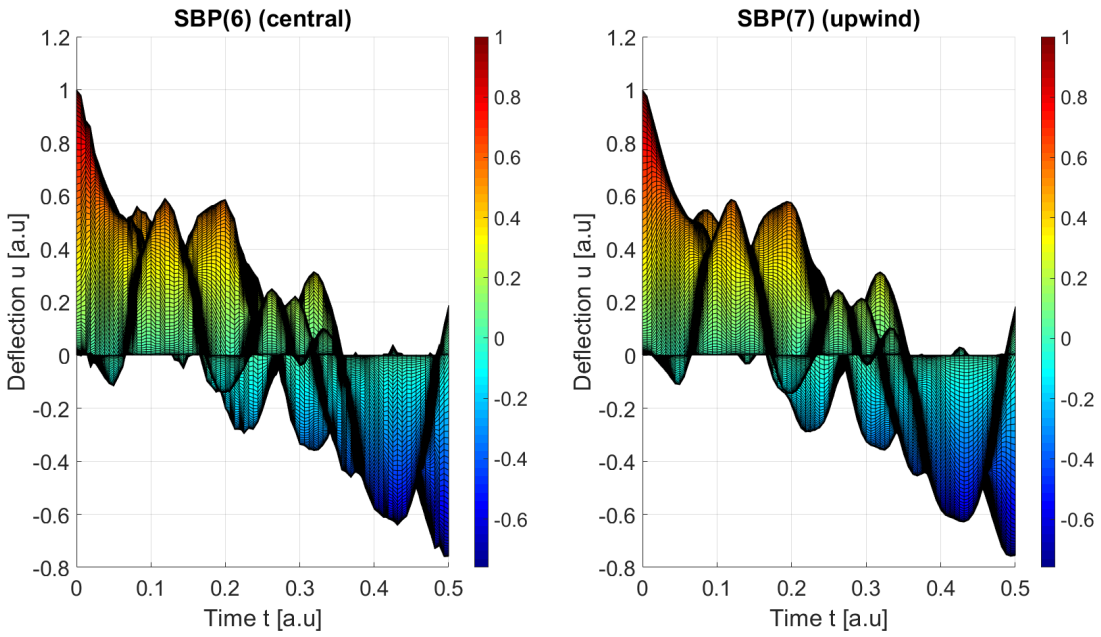

Figure 10: The numerical approximation for the dynamic beam equation (with $m = 201$ and $n = 81$) as a surface plot along the time axis. The results are shown with a 6th order accurate central SBP operator (left) and with a 7th order accurate upwind SBP operator (right), respectively.

6 Conclusions

The focus of this project has been to combine SBP operators with the projection method to develop an unconditionally stable numerical method suitable for solving stiff IVPs on first- and second-order form. The main result is that the developed method could be extended to second-order IVPs. Stability was further proved for the method when using so-called wide stencil SBP operators. Through convergence studies, a convergence rate between p and $p + 1$ was obtained for the developed method. Where p is the accuracy order of the boundary closure in the SBP operator. From the efficency study shown in Figure 7 it was seen that the developed method performs better than the explicit RK4 method, for certain stiff problems. Finally, it was seen that upwind- and central SBP operators perform similarly in terms of the l^2-error. The upwind SBP operator did however efficiently reduce spurious oscillations on problems such as the dynamic beam equation (see comparison in Figure 10).

7 Future work

To fully investigate the benefits and drawbacks of the SBP-P method, more studies need to be conducted. It is crucial to investigate the large condition number following the preconditioning and how exactly it affects the accuracy of the solution. Another subject for future work could be to extend the SBP-P method to handle nonlinear second-order IVPs. It would also be interesting to see how well the SBP-P method works, when implemented on semi-discretizations of higher-dimensional IBVPs in space. A multistage implementation of the SBP-P method should also be considered, in order to further investigate its performance.

References

[1] M. Borri et al. "Dynamic response of mechanical systems by a weak Hamiltonian formulation". In: *Journal of Computers Structures* 20 (1985), pp. 495–508. DOI: https://doi.org/10.1016/0045-7949(85)90098-7.

[2] C. L. Bottasso. "A new look at finite elements in time: a variational interpretation of Runge-Kutta methods". In: *Journal of Applied Numerical Mathematics* 25 (Dec. 1997), pp. 355–368. DOI: https://doi.org/10.1016/S0168-9274(97)00072-X.

[3] K. Mattsson. "Diagonal-norm summation by parts operators for finite difference approximations of third and fourth derivatives". In: *Journal of Computational Physics* 274 (Oct. 2014), pp. 432–454. DOI: https://doi.org/10.1016/j.jcp.2014.06.027.

[4] K. Mattsson. "Diagonal-norm upwind SBP operators". In: *Journal of Computational Physics* 335 (Apr. 2017), pp. 283–310. DOI: https://doi.org/10.1016/j.jcp.2017.01.042.

[5] K. Mattsson, M. Almquist, and M. Carpenter. "Optimal diagonal-norm SBP operators". In: *Journal of Computational Physics* 264 (May 2014), pp. 91–111. DOI: https://doi.org/10.1016/j.jcp.2013.12.041.

[6] K. Mattsson, M. Almquist, and E. van der Weide. "Boundary optimized diagonal-norm SBP operators". In: *Journal of Computational Physics* 374 (Dec. 2018), pp. 1261–1266. DOI: https://doi.org/10.1016/j.jcp.2018.06.010.

[7] K. Mattsson and J. Nordström. "Summation by parts operators for finite difference approximations of second derivatives". In: *Journal of Computational Physics* 199 (Sept. 2004), pp. 503–540. DOI: https://doi.org/10.1016/j.jcp.2004.03.001.

[8] K. Mattsson and P. Olsson. "An improved projection method". In: *Journal of Computational Physics* 372 (June 2018), pp. 349–372. DOI: https://doi.org/10.1016/j.jcp.2018.06.030.

[9] H. M. Moya-Cessa and F. Soto-Equibar. *Differential Equations: An Operational Approach*. Rinton Press, 2011.

[10] J. Nordström and T. Lundquist. "Summation-by-parts in time". In: *Journal of Computational Physics* 251 (Oct. 2013), pp. 487–499. DOI: https://doi.org/10.1016/j.jcp.2013.05.042.

[11] J. Nordström and T. Lundquist. "Summation-by-parts in Time: the Second Derivative". In: (Sept. 2014). DOI: https://doi.org/10.13140/2.1.2056.1283.

[12] P. Olsson. "Summation by parts, projections, and stability I". In: *Mathematics of Computation* 64 (July 1995), pp. 1035–1065.

[13] P. Olsson. "Summation by parts, projections, and stability II". In: *Mathematics of Computation* 64 (Oct. 1995), pp. 1473–1493. DOI: 10.1090/S0025-5718-1995-1308459-9.

8 Appendix

8.1 Appendix A: Advection-diffusion equation

8.1.1 Derivation of a continuous energy estimate

A continuous energy estimate will be derived for the advection-diffusion equation, as it is stated in (48). We start off by setting the known data to zero ($f = g_l = g_r = F = 0$) and continue by multiplying (48) by u^* from the left and integrating the result over the spatial domain to obtain

$$\int_{x_l}^{x_r} u^* u_t \mathrm{d}x + a \int_{x_l}^{x_r} u^* u_x \mathrm{d}x - \varepsilon \int_{x_l}^{x_r} u^* u_{xx} \mathrm{d}x = 0. \tag{79}$$

Adding the complex conjugate transpose of (79) to itself then leads to the expression

$$\int_{x_l}^{x_r} (u^* u_t + u_t^* u) \mathrm{d}x + a \int_{x_l}^{x_r} (u^* u_x + u_x^* u) \mathrm{d}x - \varepsilon \int_{x_l}^{x_r} (u^* u_{xx} + u_{xx}^* u) \mathrm{d}x = 0. \tag{80}$$

The third integral term in (80) may now be integrated by parts to give

$$\int_{x_l}^{x_r} (u^* u_t + u_t^* u) \mathrm{d}x + a \int_{x_l}^{x_r} (u^* u_x + u_x^* u) \mathrm{d}x + \varepsilon \int_{x_l}^{x_r} (u_x^* u_x + u_x^* u_x) \mathrm{d}x = \varepsilon \left(u^* u_x + u_x^* u \right) |_{x_l}^{x_r}. \tag{81}$$

The expression in (81) may be further simplified by using that $u^* u_x = u_x^* u$ and by using the product differentiation rule on the first and second integral terms. Doing this results in the following expression:

$$\begin{aligned} \frac{d}{dt} \|u(\cdot, t)\|^2 + 2\varepsilon \|u_x(\cdot, t)\|^2 = & -a \left(|u(x_r, t)|^2 - |u(x_l, t)|^2 \right) \\ & + 2\varepsilon \left(u^*(x_r, t) u_x^*(x_r, t) - u^*(x_l, t) u_x^*(x_l, t) \right). \end{aligned} \tag{82}$$

A continous energy estimate is then finally obtained by integrating the expression in (82) over the time domain. It is given on the form

$$\begin{aligned} \|u(\cdot, T)\|^2 + 2\varepsilon \int_{t_0}^{T} \|u_x(\cdot, t)\|^2 \mathrm{d}t = & \|u(\cdot, t_0)\|^2 - a \left(|u(x_r, t)|^2 - |u(x_l, t)|^2 \right) \\ & + 2\varepsilon \left(u^*(x_r, t) u_x^*(x_r, t) - u^*(x_l, t) u_x^*(x_l, t) \right). \end{aligned} \tag{83}$$

8.1.2 Derivation of a discrete energy estimate

A discrete energy estimate will be derived for the SBP-P implementation defined in (52) on the advection-diffusion equation stated as in (48). During the derivation, the notation defined in (53) will be used. We may start off by setting all known data to zero ($f = g_l = g_r = F = 0$) and continue by multiplying (52) by $w^*(H_t \otimes H_x)$ from the left to obtain

$$\begin{aligned} w^*(H_t P_t D_{(t)} P_t \otimes H_x) w = & - a w^*(H_t P_t \otimes H_x P_x D P_x) w \\ & + \varepsilon w^*(H_t P_t \otimes H_x P_x D_2 P_x) w \\ & - \sigma_x w^*(H_t P_t \otimes H_x (I_m - P_x)) w \\ & - \sigma_t w^*(H_t (I_n - P_t) \otimes H_x) w. \end{aligned} \tag{84}$$

The properties of the projection operator $HP = P^T H$ and $P = P^2$ may now be used to rewrite the expression in (84) in terms of the projected and fully projected solution as

$$\begin{aligned} \tilde{w}^*(H_t D_{(t)} \otimes H_x) \tilde{w} = & - a \tilde{\tilde{w}}^*(H_t \otimes H_x D) \tilde{\tilde{w}} \\ & + \varepsilon \tilde{\tilde{w}}^*(H_t \otimes H_x D_2) \tilde{\tilde{w}} \\ & - \sigma_x \tilde{w}^*(H_t \otimes H_x (I_m - P_x)) \tilde{w} \\ & - \sigma_t w^*(H_t (I_n - P_t) \otimes H_x) w. \end{aligned} \tag{85}$$

Now, adding the complex conjugate transpose of the expression in (85) and combining terms leads to

$$\begin{aligned}\tilde{w}^*\left(\left[H_tD_{(t)}+D_{(t)}^TH_t\right]\otimes H_x\right)\tilde{w} =& -a\tilde{\tilde{w}}^*\left(H_t\otimes\left[H_xD+D^TH_x\right]\right)\tilde{\tilde{w}}\\ &+\varepsilon\tilde{\tilde{w}}^*\left(H_t\otimes\left[H_xD_2+D_2^TH_x\right]\right)\tilde{\tilde{w}}\\ &-2\sigma_x\tilde{w}^*\left(H_t\otimes H_x(I_m-P_x)\right)\tilde{w}\\ &-2\sigma_t w^*\left(H_t(I_n-P_t)\otimes H_x\right)w.\end{aligned} \tag{86}$$

Let us handle the terms separately, by introducing the following variables for the expression in (86):

$$\begin{aligned}\text{(I)} =& \text{(II)}\\ &+\text{(III)}\\ &+\text{(IV)}\\ &+\text{(V)}.\end{aligned} \tag{87}$$

Starting with the first term in the l.h.s., we may use Lemma 4.1 and 4.2 to directly rewrite it as follows:

$$\begin{aligned}&\text{(central } D_1\text{)}: \quad \text{(I)} = \|\tilde{w}^{(n)}\|_{H_x}^2-\|\tilde{w}^{(0)}\|_{H_x}^2,\\ &\text{(upwind } D_-\text{)}: \quad \text{(I)} = \|\tilde{w}^{(n)}\|_{H_x}^2-\|\tilde{w}^{(0)}\|_{H_x}^2-\frac{1}{2}\tilde{w}^*\left(S\otimes H_x\right)\tilde{w}.\end{aligned} \tag{88}$$

In space we have used central SBP operators exclusively. This means that for the variables (II) and (III), the operators D and D_2 are central SBP operators. The first variable (II) is then treated similarly to (I), by using Lemma 4.1. The resulting expression is then given as

$$\text{(II)} = -a\left(\|\tilde{\tilde{w}}_m\|_{H_t}^2-\|\tilde{\tilde{w}}_0\|_{H_t}^2\right). \tag{89}$$

For the third variable (III), we need to introduce two properties of the second derivative central SBP operator D_2 in accordance with [7]:

$$\begin{aligned}&H_xD_2+D_2^TH_x = -2M-e_1d_1-d_1^Te_1^T+e_md_m+d_m^Te_m^T,\\ &M=M^T=D_1^TH_xD_1\geq 0,\end{aligned} \tag{90}$$

where $d_i=e_i^TD_1$ is a first derivative approximation at the ith grid point. Using these properties, the variable (III) may be rewritten as follows:

$$\begin{aligned}\text{(III)} &= \varepsilon\tilde{\tilde{w}}^*\left(H_t\otimes\left[H_xD_2+D_2^TH_x\right]\right)\tilde{\tilde{w}}\\ &= -2\varepsilon\tilde{\tilde{w}}^*\left(H_t\otimes D_1^TH_xD_1\right)\tilde{\tilde{w}}\\ &-\varepsilon\tilde{\tilde{w}}^*\left(H_t\otimes e_0d_0\right)\tilde{\tilde{w}}-\varepsilon\tilde{\tilde{w}}^*\left(H_t\otimes d_0^Te_0^T\right)\tilde{\tilde{w}}\\ &+\varepsilon\tilde{\tilde{w}}^*\left(H_t\otimes e_md_m\right)\tilde{\tilde{w}}+\varepsilon\tilde{\tilde{w}}^*\left(H_t\otimes d_m^Te_m^T\right)\tilde{\tilde{w}}\\ &= -2\varepsilon\left((I_n\otimes D_1)\tilde{\tilde{w}}\right)^*\left(H_t\otimes H_x\right)(I_n\otimes D_1)\tilde{\tilde{w}}\\ &-\varepsilon\left((I_n\otimes e_0^T)\tilde{\tilde{w}}\right)^*H_t(I_n\otimes d_0)\tilde{\tilde{w}}-\varepsilon\left((I_n\otimes d_0)\tilde{\tilde{w}}\right)^*H_t(I_n\otimes e_0^T)\tilde{\tilde{w}}\\ &+\varepsilon\left((I_n\otimes e_m^T)\tilde{\tilde{w}}\right)^*H_t(I_n\otimes d_m)\tilde{\tilde{w}}+\varepsilon\left((I_n\otimes d_m)\tilde{\tilde{w}}\right)^*H_t(I_n\otimes e_m^T)\tilde{\tilde{w}}\\ &= -2\varepsilon\|\left(\tilde{\tilde{w}}\right)_x\|_{H_t\otimes H_x}^2-\varepsilon\tilde{\tilde{w}}_0^*H_t\left(\tilde{\tilde{w}}_0\right)_x-\varepsilon\left(\tilde{\tilde{w}}_0\right)_x^*H_t\tilde{\tilde{w}}_0+\varepsilon\tilde{\tilde{w}}_m^*H_t\left(\tilde{\tilde{w}}_m\right)_x+\varepsilon\left(\tilde{\tilde{w}}_m\right)_x^*H_t\tilde{\tilde{w}}_m.\end{aligned} \tag{91}$$

The fourth and fifth variables (IV) and (V) are rewritten similarly by using the definition of the projection operator P. The definition is given as

$$P\equiv I-H^{-1}L\left(L^TH^{-1}L\right)^{-1}L^T, \tag{92}$$

which then makes it possible to rewrite $H(I-P)$ as follows:

$$\begin{aligned}H(I-P) &= H\left(I-I+H^{-1}L\left(L^TH^{-1}L\right)^{-1}L^T\right)\\ &= L\left(L^TH^{-1}L\right)^{-1}L^T.\end{aligned} \tag{93}$$

Using the result of (93) then makes it possible to rewrite (IV) and (V) on the following form:

$$\begin{aligned}
\text{(IV)} &= -2\sigma_x \tilde{w}^* \left(H_t \otimes H_x (I_m - P_x)\right) \tilde{w} \\
&= -2\sigma_x \left((I_n \otimes L_x^T)\tilde{w}\right)^* \left(H_t \otimes \left(L_x^T H_x^{-1} L_x\right)^{-1}\right) (I_n \otimes L_x^T)\tilde{w}, \\
\text{(V)} &= -2\sigma_t w^* \left(H_t (I_n - P_t) \otimes H_x\right) w \\
&= -2\sigma_t \left((L_t^T \otimes I_m)w\right)^* \left(\left(L_t^T H_t^{-1} L_t\right)^{-1} \otimes H_x\right) (L_t^T \otimes I_m)w.
\end{aligned} \tag{94}$$

By recombining all the derived variables leads to the following discrete energy estimate:

$$\begin{aligned}
&\text{(central } D_1\text{)}: \qquad 2\varepsilon \|(\tilde{\tilde{w}})_x\|^2_{H_t \otimes H_x} = IC_h + BC_h + PT_h, \\
&\text{(upwind } D_-\text{)}: \qquad 2\varepsilon \|(\tilde{\tilde{w}})_x\|^2_{H_t \otimes H_x} = IC_h + BC_h + PT_h + AD_h,
\end{aligned} \tag{95}$$

where the initial condition terms IC_h, the boundary condition terms BC_h, the penalty terms PT_h and the artifical damping term AD_h are given as follows:

$$\begin{aligned}
IC_h &= -\|\tilde{w}^{(n)}\|^2_{H_x} + \|\tilde{w}^{(0)}\|^2_{H_x}, \\
BC_h &= -a\left(\|\tilde{\tilde{w}}_m\|^2_{H_t} - \|\tilde{\tilde{w}}_0\|^2_{H_t}\right) + \varepsilon\left(\tilde{\tilde{w}}_m^* H_t (\tilde{\tilde{w}}_m)_x + (\tilde{\tilde{w}}_m)_x^* H_t \tilde{\tilde{w}}_m - \tilde{\tilde{w}}_0^* H_t (\tilde{\tilde{w}}_0)_x - (\tilde{\tilde{w}}_0)_x^* H_t \tilde{\tilde{w}}_0\right), \\
PT_h &= -2\sigma_x \left((I_n \otimes L_x^T)\tilde{w}\right)^* \left(H_t \otimes (L_x^T H_x^{-1} L_x)^{-1}\right) (I_n \otimes L_x^T)\tilde{w} \\
&\quad -2\sigma_t \left((L_t^T \otimes I_m)w\right)^* \left((L_t^T H_t^{-1} L_t)^{-1} \otimes I_m\right) (L_t^T \otimes I_m)w, \\
AD_h &= \frac{1}{2}\tilde{w}^* (S \otimes H_x)\, \tilde{w}.
\end{aligned} \tag{96}$$

8.2 Appendix B: Dynamic beam equation

8.2.1 Derivation of a continuous energy estimate

A continuous energy estimate will be derived for the dynamic beam equation, as it is stated in (69). We start off by setting the known data to zero ($f = g_l = g_r = F = 0$) and continue by multiplying (69) by u_t^* from the left and integrating the result over the spatial domain to obtain

$$\int_{x_l}^{x_r} u_t^* u_{tt} \mathrm{d}x + \alpha \int_{x_l}^{x_r} u_t^* u_{xxxx} \mathrm{d}x = 0. \tag{97}$$

Adding the complex conjugate transpose of (97) to itself then leads to the expression

$$\int_{x_l}^{x_r} (u_t^* u_{tt} + u_{tt}^* u_t) \mathrm{d}x + \alpha \int_{x_l}^{x_r} (u_t^* u_{xxxx} + u_{xxxx}^* u_{tt}) \mathrm{d}x = 0. \tag{98}$$

By using the product differentiation rule on the first integral and integrating the second integral term by parts twice then leads to the following expression for the energy rate:

$$\begin{aligned}
\frac{d}{dt}\left(\|u_t(\cdot,t)\|^2 + \alpha \|u_{xx}(\cdot,t)\|^2\right) =& 2\alpha \left(u_{tx}^*(x_r,t) u_{xx}(x_r,t) - u_{tx}^*(x_l,t) u_{xx}(x_l,t)\right) \\
&- 2\alpha \left(u_t^*(x_r,t) u_{xxx}(x_r,t) - u_t^*(x_l,t) u_{xxx}(x_l,t)\right).
\end{aligned} \tag{99}$$

By now integrating the energy rate expression in (99) leads to the following continuous energy estimate:

$$\begin{aligned}
\|u_t(\cdot,T)\|^2 + \alpha \|u_{xx}(\cdot,T)\|^2 =& \|u_t(\cdot,t_0)\|^2 + \alpha \|u_{xx}(\cdot,t_0)\|^2 \\
&+ 2\alpha \int_{t_0}^{T} (u_{tx}^*(x_r,t) u_{xx}(x_r,t) - u_{tx}^*(x_l,t) u_{xx}(x_l,t)) \mathrm{d}t \\
&- 2\alpha \int_{t_0}^{T} (u_t^*(x_r,t) u_{xxx}(x_r,t) - u_t^*(x_l,t) u_{xxx}(x_l,t)) \mathrm{d}t.
\end{aligned} \tag{100}$$

8.2.2 Derivation of a discrete energy estimate

A discrete energy estimate will be derived for the SBP-P implementation defined in (74) on the dynamic beam equation stated as in (69). During the derivation, the notation defined in (53) will be used. We may start off by setting all known data to zero ($f = g_l = g_r = F = 0$) and continue by multiplying (74) by $w^*(I_n \otimes H_x)$ from the left to obtain

$$\begin{aligned} w^* \left(P_t^T D_{(t)}^T H_t D_{(t)} D_{(t)} P_t \otimes H_x \right) w = &-\alpha w^* \left(P_t^T D_{(t)}^T H_t P_t \otimes H_x P_x D_4 P_x \right) w \\ &- \sigma_x w^* \left(P_t^T D_{(t)}^T H_t P_t \otimes H_x (I_m - P_x) \right) w \\ &- \frac{\sigma_t}{k} w^* \left(H_t (I_n - P_t) \otimes H_x \right) w, \end{aligned} \tag{101}$$

where we may rewrite the expression in equation (101) in terms of the projected and fully projected solution as:

$$\begin{aligned} \tilde{w}^* \left(D_{(t)}^T H_t D_{(t)} D_{(t)} \otimes H_x \right) \tilde{w} = &-\alpha \tilde{\tilde{w}}^* \left(D_{(t)}^T H_t \otimes H_x D_4 \right) \tilde{\tilde{w}} \\ &- \sigma_x \tilde{w}^* \left(D_{(t)}^T H_t \otimes H_x (I_m - P_x) \right) \tilde{w} \\ &- \frac{\sigma_t}{k} w^* \left(H_t (I_n - P_t) \otimes H_x \right) w. \end{aligned} \tag{102}$$

Now, introducing the discrete time derivative as $(\cdot)_t \equiv (D_{(t)} \otimes I_m)(\cdot)$ and adding the complex conjugate transpose of the expression in (102) to itself and grouping together terms (as much as possible) leads to

$$\begin{aligned} \tilde{w}_t^* \left([H_t D_{(t)} + D_{(t)}^T H_t] \otimes H_x \right) \tilde{w}_t = &-\alpha \left(\tilde{\tilde{w}}^* \left(D_{(t)}^T H_t \otimes H_x D_4 \right) \tilde{\tilde{w}} + \tilde{\tilde{w}}^* \left(H_t D_{(t)} \otimes D_4^T H_x \right) \tilde{\tilde{w}} \right) \\ &- \sigma_x \tilde{w}^* \left([D_{(t)}^T H_t + H_t D_{(t)}] \otimes H_x (I_m - P_x) \right) \tilde{w} \\ &- \frac{2\sigma_t}{k} w^* \left(H_t (I_n - P_t) \otimes H_x \right) w. \end{aligned} \tag{103}$$

Let us handle the terms separately, by introducing the following variables for the expression in (103):

$$\begin{aligned} \text{(i)} = &\text{(ii)} \\ &+ \text{(iii)} \\ &+ \text{(iv)}\,. \end{aligned} \tag{104}$$

For the variables (i) and (iii), we may use Lemma 4.1 and 4.2 to rewrite them as follows:

$$\begin{aligned} &\text{(central } D_1\text{)}: \quad \text{(i)} = \|\tilde{w}_t^{(n)}\|_{H_x}^2 - \|\tilde{w}_t^{(0)}\|_{H_x}^2, \\ &\text{(upwind } D_-\text{)}: \quad \text{(i)} = \|\tilde{w}_t^{(n)}\|_{H_x}^2 - \|\tilde{w}_t^{(0)}\|_{H_x}^2 - \frac{1}{2} \tilde{w}_t^* \left(S \otimes H_x \right) \tilde{w}_t, \end{aligned} \tag{105}$$

and

$$\begin{aligned} \text{(iii)} = &-\sigma_x \left(L_x^T \tilde{w}^{(n)} \right)^* \left(L_x^T H_x^{-1} L_x \right)^{-1} L_x^T \tilde{w}^{(n)} \\ &+ \sigma_x \left(L_x^T \tilde{w}^{(0)} \right)^* \left(L_x^T H_x^{-1} L_x \right)^{-1} L_x^T \tilde{w}^{(0)} \\ &+ \sigma_x \left((I_n \otimes L_x^T) \tilde{w} \right)^* \left(S \otimes \left(L_x^T H_x^{-1} L_x \right)^{-1} \right) (I_n \otimes L_x^T) \tilde{w}, \end{aligned} \tag{106}$$

where $S = 0$ if a central operator has been used. For the second term (ii), we need to introduce two properties of the fourth derivative central SBP operator D_4 in accordance with [3]:

$$\begin{aligned} &H_x D_4 = N - e_0 d_{3:0} + e_m d_{3:m} + d_{1:0}^T d_{2:0} - d_{1:m}^T d_{2:m}, \\ &N = N^T > 0, \end{aligned} \tag{107}$$

where $d_{3:i} = e_i^T D_3$ is a third derivative approximation, $d_{2:i} = e_i^T D_2$ is a second derivative approximation and $d_{1:i} = e_i^T D_1$ is a first derivative approximation at the ith grid point. In addition to the notation presented in Appendix 8.1, we define a discrete second derivative at the boundary points as $(w_i)_{xx} \equiv (I_n \otimes d_{2:i})w$. Similarly a discrete third derivative at the boundary points is given as $(w_i)_{xxx} \equiv (I_n \otimes d_{3:i})w$. Using these properties of the SBP operator D_4 and the introduced notation, the variable (ii) may be written as

$$\begin{aligned}
\text{(ii)} &= -\alpha \left(\|\tilde{\tilde{w}}^{(n)}\|_N^2 - \|\tilde{\tilde{w}}^{(0)}\|_N^2 \right) \\
&\quad + 2\alpha \left(\left(D_{(t)}\tilde{\tilde{w}}_0\right)^* H_t \left(\tilde{\tilde{w}}_0\right)_{xxx} - \left(D_{(t)}\tilde{\tilde{w}}_m\right)^* H_t \left(\tilde{\tilde{w}}_m\right)_{xxx} \right) \\
&\quad - 2\alpha \left(\left(D_{(t)}\tilde{\tilde{w}}_0\right)_x^* H_t \left(\tilde{\tilde{w}}_0\right)_{xx} - \left(D_{(t)}\tilde{\tilde{w}}_m\right)_x^* H_t \left(\tilde{\tilde{w}}_m\right)_{xx} \right) \\
&= -\alpha \left(\|\tilde{\tilde{w}}^{(n)}\|_N^2 - \|\tilde{\tilde{w}}^{(0)}\|_N^2 \right) \\
&\quad + 2\alpha \left(\left(\tilde{\tilde{w}}_0\right)_t^* H_t \left(\tilde{\tilde{w}}_0\right)_{xxx} - \left(\tilde{\tilde{w}}_m\right)_t^* H_t \left(\tilde{\tilde{w}}_m\right)_{xxx} \right) \\
&\quad - 2\alpha \left(\left(\tilde{\tilde{w}}_0\right)_{tx}^* H_t \left(\tilde{\tilde{w}}_0\right)_{xx} - \left(\tilde{\tilde{w}}_m\right)_{tx}^* H_t \left(\tilde{\tilde{w}}_m\right)_{xx} \right).
\end{aligned} \tag{108}$$

The remaining term (iv) corresponds exactly to the term (V) in (94) (scaled by $1/k^2$). Now, by combining all terms (i − iv) leads to the following discrete energy estimate:

$$\begin{aligned}
&\text{(central } D_1\text{)}: && \|\tilde{\tilde{w}}_t^{(n)}\|_{H_x}^2 + \alpha \|\tilde{\tilde{w}}^{(n)}\|_N^2 = \|\tilde{\tilde{w}}_t^{(0)}\|_{H_x}^2 + \alpha \|\tilde{\tilde{w}}^{(0)}\|_N^2 + BC_h + PT_h, \\
&\text{(upwind } D_-\text{)}: && \|\tilde{\tilde{w}}_t^{(n)}\|_{H_x}^2 + \alpha \|\tilde{\tilde{w}}^{(n)}\|_N^2 = \|\tilde{\tilde{w}}_t^{(0)}\|_{H_x}^2 + \alpha \|\tilde{\tilde{w}}^{(0)}\|_N^2 + BC_h + AD_h + PT_h,
\end{aligned} \tag{109}$$

where BC_h, AD_h and PT_h are given by:

$$\begin{aligned}
BC_h &= 2\alpha \left(\left(\tilde{\tilde{w}}_m\right)_{tx}^* H_t \left(\tilde{\tilde{w}}_m\right)_{xx} - \left(\tilde{\tilde{w}}_m\right)_t^* H_t \left(\tilde{\tilde{w}}_m\right)_{xxx} \right) \\
&\quad - 2\alpha \left(\left(\tilde{\tilde{w}}_0\right)_{tx}^* H_t \left(\tilde{\tilde{w}}_0\right)_{xx} - \left(\tilde{\tilde{w}}_0\right)_t^* H_t \left(\tilde{\tilde{w}}_0\right)_{xxx} \right), \\
AD_h &= \frac{1}{2} \tilde{\tilde{w}}_t^* \left(S \otimes H_x\right) \tilde{\tilde{w}}_t + \frac{1}{2} \tilde{\tilde{w}}^* \left(S \otimes N\right) \tilde{\tilde{w}} \\
&\quad + \sigma_x \left((I_n \otimes L_x^T)\tilde{w} \right)^* \left(S \otimes \left(L_x^T H_x^{-1} L_x \right)^{-1} \right) (I_n \otimes L_x^T)\tilde{w}, \\
PT_h &= -\sigma_x \left\{ \left(L_x^T \tilde{w}^{(n)} \right)^* \left(L_x^T H_x^{-1} L_x \right)^{-1} L_x^T \tilde{w}^{(n)} - \left(L_x^T \tilde{w}^{(0)} \right)^* \left(L_x^T H_x^{-1} L_x \right)^{-1} L_x^T \tilde{w}^{(0)} \right\} \\
&\quad - \frac{\sigma_t}{k} \left((L_t^T \otimes I_m)w \right)^* \left((L_t^T H_t^{-1} L_t)^{-1} \otimes H_x \right) (L_t^T \otimes I_m)w.
\end{aligned} \tag{110}$$